WILEY

SmartBot

REVIEW ARTICLE OPEN ACCESS

Magnetic Continuum Robot for Intelligent Manipulation in Medical Applications

Yuanbiao Ma[1] | Xuanyu An[1] | Qijun Yang[1] | Mingxue Cai[2] | Zhiqiang Tang[3] | Jinke Chang[4,5] | Veronica Iacovacci[6,7] | Tiantian Xu[2] | Li Zhang[8,9,10] | Qianqian Wang[1]

[1]Jiangsu Key Laboratory for Design and Manufacture of Micro-Nano Biomedical Instruments, School of Mechanical Engineering, Southeast University, Nanjing, China | [2]Guangdong Provincial Key Laboratory of Robotics and Intelligent System, Shenzhen Institute of Advanced Technology, Chinese Academy of Sciences, Shenzhen, China | [3]Department of Mechanical Engineering, National University of Singapore, Queenstown, Singapore | [4]Department of Engineering Science, University of Oxford, Oxford, UK | [5]Department of Surgical Biotechnology, Division of Surgery & Interventional Science, Centre for Biomaterials in Surgical Reconstruction and Regeneration, University College London, London, UK | [6]BioRobotics Institute, Scuola Superiore Sant'Anna, Pisa, Italy | [7]Department of Excellence in Robotics & AI, Scuola Superiore Sant'Anna, Pisa, Italy | [8]Department of Mechanical and Automation Engineering, The Chinese University of Hong Kong, Hong Kong, China | [9]Chow Yuk Ho Technology Center for Innovative Medicine, The Chinese University of Hong Kong, Hong Kong, China | [10]Multi-Scale Medical Robotics Center, Hong Kong Science Park, Hong Kong, China

Correspondence: Qianqian Wang (qqwang@seu.edu.cn) | Tiantian Xu (tt.xu@siat.ac.cn) | Li Zhang (lizhang@cuhk.edu.cn)

Received: 26 December 2024 | **Revised:** 24 February 2025 | **Accepted:** 7 March 2025

Funding: The authors thank the financial support from the National Natural Science Foundation of China (No. 52205590), the Natural Science Foundation of Jiangsu Province (No. BK20220834), the Start-up Research Fund of Southeast University (No. RF1028623098), the Taihu Lake Innovation Fund for the School of Future Technology of Southeast University, and in part by SIAT-CUHK Joint Laboratory of Robotics and Intelligent Systems. Funded by the European Union. Views and opinions expressed are however those of the authors only and do not necessarily reflect those of the European Union or the European Research Council Executive Agency. Neither the European Union nor the granting authority can be held responsible for them. This work is supported by ERC grant (I-BOT, 101162939).

Keywords: intelligent manipulation | magnetic actuation | magnetic continuum robot | medical application

ABSTRACT

Magnetic continuum robots (MCRs) have garnered substantial attention as a new class of flexible robotic systems capable of navigating complex and confined spaces with remarkable dexterity. By combining continuous, deformable structures with remotely applied magnetic fields, MCRs achieve contactless, remote manipulation, making them well-suited for medical applications. This review introduces recent advances in MCR research, focusing on design principles, structural configurations, and control strategies. Various MCR designs and structures, including those integrated with permanent magnets, magnetic matter, ferromagnetic sphere, and micro coil, are discussed. Furthermore, different magnetic actuation platforms are introduced, and the level of MCR automation is classified based on control strategies. Key intelligent manipulation capabilities of MCRs, including navigation, delivery, printing, grasping, imaging, and sensing are explored. Finally, future development priorities and directions are identified to provide insights for advancing intelligent robotic systems.

1 | Introduction

Continuum robots (CRs) demonstrate exceptional adaptability and precision in navigating complex environments, enabling tasks beyond the capabilities of traditional rigid-link robots [1, 2]. Unlike traditional rigid-link robots, CRs inherently possess compliance and dexterity, enabling them to navigate intricate environments, execute complex tasks, and interact safely with various objects. These distinctive characteristics make CRs particularly promising in the medical field [3–7]. Among the

Yuanbiao Ma and Xuanyu An contributed equally to this work.

various actuation methods developed for CRs, magnetic actuation has garnered considerable attention due to its distinctive ability to provide contactless and wireless control. Conventional actuation techniques, such as pneumatic [8, 9], hydraulic [10–13], or tendon-driven systems [14–16], often encounter limitations related to bulkiness, restricted workspace, and mechanical complexity. In contrast, magnetic actuation offers a remote and secure solution by utilizing external magnetic fields to control robot embedded with magnetic components. This approach enables remote in situ manipulation of CRs and is suitable for navigation in narrow, tortuous passages that are difficult to reach. Magnetic actuation methods, which are now widely used to control and actuate microrobots [17–21]. Furthermore, combined with imaging systems, the potential for medical applications of microrobots is further enhanced [22–26]. The continuous advancements in magnetic actuation techniques and the development of integrated magnetic actuation systems have substantially improved the precision of control and real-time tracking capabilities of MCRs, thereby establishing a foundation for their clinically intelligent manipulations.

MCRs integrate the principles of magnetic actuation with the flexibility of continuum structures, resulting in robotic systems that exhibit excellent adaptability and functionality. MCRs have demonstrated significant potential across various intelligent applications, especially within the medical field [27–31]. Their capability to traverse complex anatomical pathways and perform delicate manipulations facilitates MCRs as a promising technology for advancing future biomedical devices. However, the advancement of MCRs is accompanied by several challenges that necessitate further research and innovation. The design and structural configuration of MCRs play a vital role in determining their performance and versatility, with components such as the use of permanent magnet, magnetic matter, ferromagnetic sphere, and micro coil giving their magnetism. Additionally, the integration of sensing capabilities and real-time feedback mechanisms is essential for enabling intelligent manipulation, as MCRs must adapt to unpredictable environments and execute complex tasks autonomously or semi-autonomously.

As illustrated in Figure 1, different designs and structures, as well as the integration of functional components give MCRs a more diverse range of functions. The incorporation of imaging technology and control algorithms further enables intelligent manipulation, expanding their applications in the medical field. This review aims to provide a comprehensive overview of the current state of research on magnetic continuum robots for intelligent manipulation, focusing on critical aspects of MCR design principles, structural configurations, and control strategies while providing a comparison. Based on the current state-of-the-art research and development trends in MCRs, we finally discuss the future research directions and perspective.

2 | Design and Structure of MCR

This section will introduce various designs and structures of MCRs for intelligent manipulation, focusing on their integration with different magnetic components. MCRs integrated with permanent magnets will be introduced, which utilize the stable magnetic field generated by permanent magnets to provide consistent actuation force and torque, enabling remote control. Next, MCRs integrated with magnetic matter (e.g., magnetic particles) will be discussed, where the response of flexible magnetic segment to the magnetic field enables finer and more complex manipulation. Following this, MCRs integrated with ferromagnetic spheres will be presented, which enhance the robot's movement flexibility and operational precision by controlling the position and orientation of ferromagnetic spheres under magnetic resonance imaging (MRI). Finally, MCRs integrated with micro coils will be explored, as this design leverages electromagnetic fields to achieve high-precision positioning and control. Table 1 presents the key characteristics and application scenario of representative MCRs, highlighting variations arising

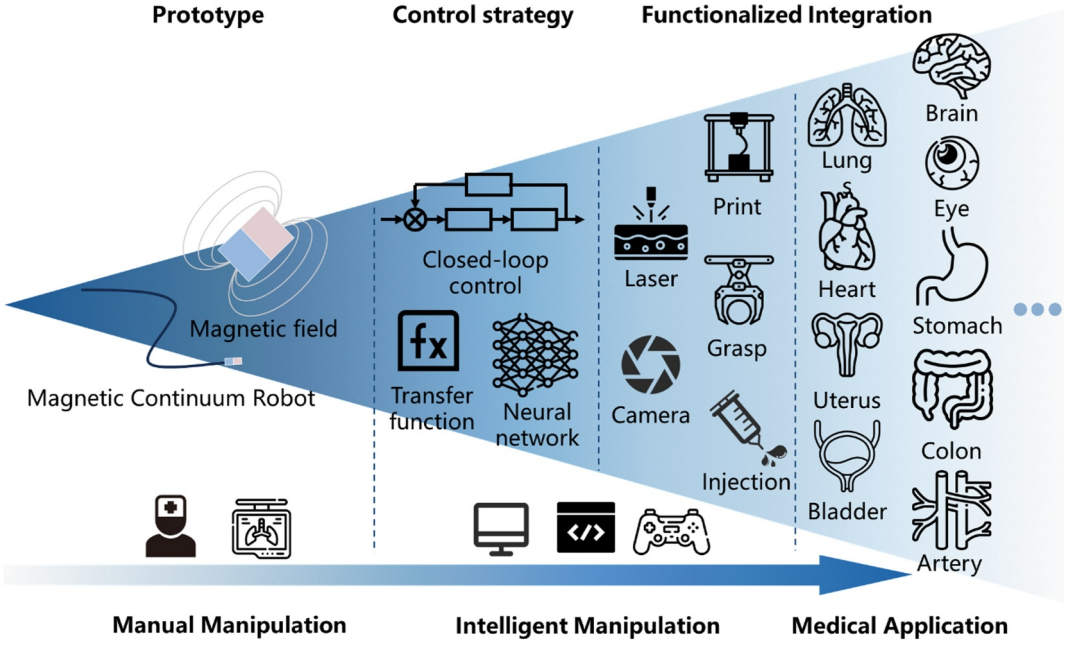

FIGURE 1 | Manipulation and application scenarios of magnetic continuum robots.

TABLE 1 | Characteristics and application scenario of different magnetic continuum robots.

Ref	Application	Magnetization component	Actuation source	Diameter of magnetic part	Length of magnetic part	Workspace	Validation experiment condition	Unique design	Advantages
[32]	Stroke treatment	Permanent magnet	Electromagnetic actuation	800 μm	14 mm	200 × 200 × 400 mm	Human vascular model Ex vivo human placenta model In vivo porcine model	Helical protrusion Articulating magnetic tip	Pushability limitations addressed by rotating the MCR Navigation in the artery achieved by active magnetic deflection
[33]	Minimally invasive surgery	Permanent magnet	Permanent magnet	400 μm	21 mm	Within 40 mm × 40 mm	Eye phantom	Embedded with two opposite axially polarized magnets	Deformation of higher order curve under the external magnetic field
[34]	Neurosurgery	Magnetic particles	Permanent magnet	600 μm	3 mm	—	Cerebrovascular phantom Carotid artery phantom	Hydrogel skins Hard magnetic particles embedded in soft polymer matrix	Significant reduction in friction Flexible and programmable magnetization
[35]	Endovascular surgery	Magnetic particles	Permanent magnet	1.9 mm	2.5 mm	700 × 500 × 500 mm	Vascular phantom	Magnetic tip consists of Ecoflex 00–30 and NdFeB	Wide range of deflection angle Programmable magnetization
[36]	Minimally invasive endovascular interventions	Ferromagnetic sphere	MRI	2 mm	2 mm	—	Vessel phantom Porcine aorta	Endovascular catheter was designed with a spherical ferromagnetic tip	Real-time imaging, localization and magnetic navigation are achieved under a MR system
[37]	Catheterization procedures	Ferromagnetic sphere	MRI	4.5 mm	32.7 mm	—	In vitro	Magnetic tip with two ferromagnetic spheres	Improved deflection performance under MRI system
[38]	Endovascular catheterization procedures	Micro coil	MRI	2 mm	7 mm	—	Vascular phantom	Hand-wound solenoid coil at the distal tip	Current-controlled to flexibly adjust the deflection direction to accommodate different branches
[39]	Aneurysm embolization	Micro coil	MRI	1 mm	3 mm	—	In vitro Ex vivo Kidney Neurovascular phantom	Quad-configuration micro coils	Diameter of magnetic catheter and coil power consumption are reduced

from different design principles. Through the analysis of these four distinct designs, this section will highlight the potential and advantages of MCRs in intelligent manipulation.

2.1 | MCR Integrated With Permanent Magnet

MCRs integrated with permanent magnets offer several key advantages, including enhanced stability, simplicity of control, and high efficiency. Permanent magnets, with their efficient and stable magnetic properties, provide essential support for the intelligent manipulation of magnetic continuum robots in complex environments. In MCRs, Neodymium iron boron (NdFeB) magnet is commonly used as a permanent magnetic material to impart magnetism to the tip of a catheter or guidewire [40–44]. The magnetic catheter and guidewire can be actively deflected under an external magnetic field, enabling manipulation in confined environments.

Based on the basic magnetic continuum robot, Dreyfus et al. adopted a unique locomotion modality [32]. It involves incorporating a helical protrusion on the robot's surface and combining insertion with rotation (Figure 2a). Functioning like a flexible screw, the protrusion engages the vessel wall, effectively pulling robot forward upon rotation. Furthermore, the robot features a segmented, articulating magnetic tip design. This design ensures that the tip remains soft and atraumatic while maximizing the achievable deflection angle. Integration of two or more permanent magnets with a MCR enhances its maneuverability [45–48]. Jeon et al. designed and fabricated a soft MCR, which integrated

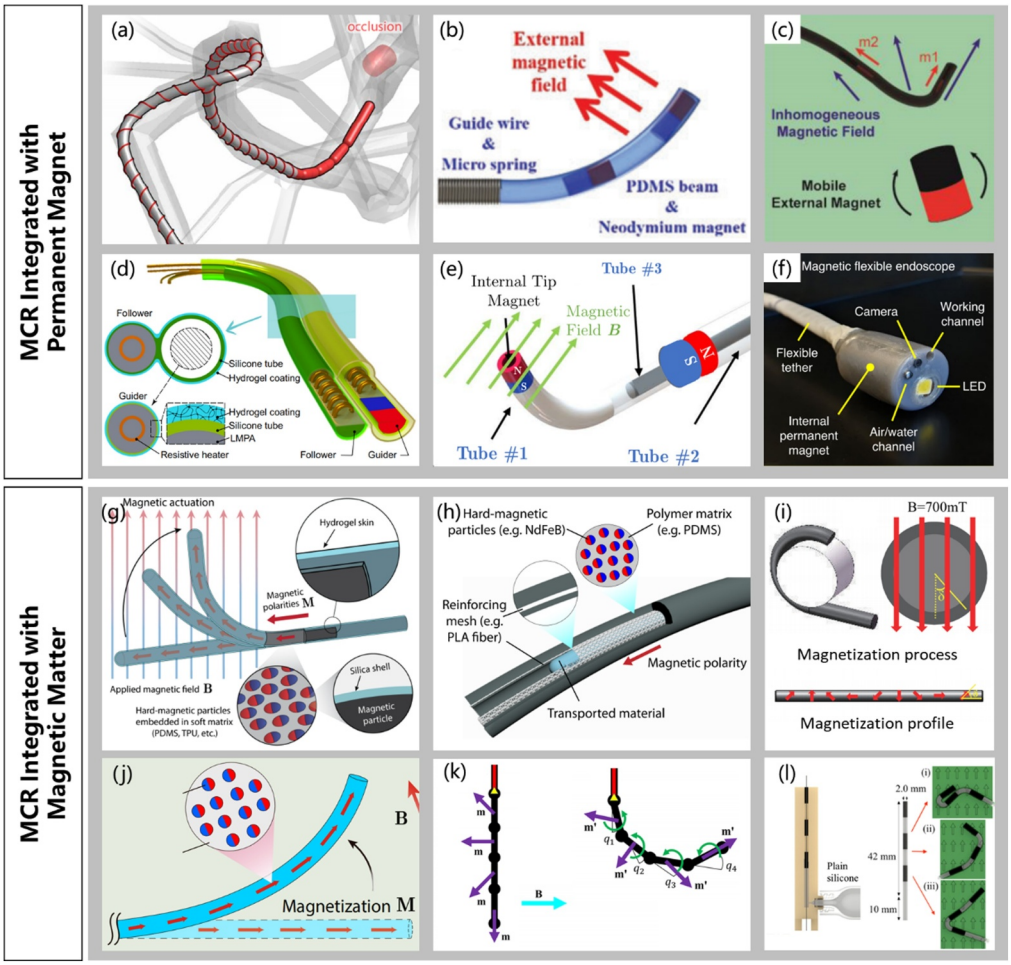

FIGURE 2 | MCRs integrated with permanent magnet and magnetic matter. (a–f) MCRs integrated with permanent magnet: (a) Permanent MCR with articulated magnetic tip. Reproduced with permission [32]. Copyright 2024, AAAS. (b) MCR integrated with two permanent magnets. Reproduced with permission [49]. Copyright 2019, Mary Ann Liebert. (c) MCR integrated with two opposite permanent magnets. Reproduced with permission [50]. Copyright 2021, IEEE. (d) Millimeter-scale MCR embedded tiny permanent magnet. Reproduced with permission [51]. Copyright 2024, The Authors. (e) Concentric tube MCR integrated with multiple permanent magnets. Reproduced with permission [55]. Copyright 2024, IEEE. (f) Robotic magnetic flexible endoscope. Reproduced with permission [57]. Copyright 2020, Springer Nature. (g–l) MCRs integrated with magnetic matter: (g) Ferromagnetic soft continuum robot with hydrogel skins. Reproduced with permission [34]. Copyright 2019, AAAS. (h) Ferromagnetic soft catheter robot composed of soft polymer matrix. Reproduced with permission [66]. Copyright 2021, The Authors. (i) Magnetization process and magnetization profile of magnetic steerable guidewire. Reproduced with permission [35]. Copyright 2022, IEEE. (j) Magnetic soft continuum robot with hard magnetic particles dispersed in the polymer matrix. Reproduced with permission [68]. Copyright 2021, PNAS. (k) Magnetically actuated coiling soft robot with variable stiffness. Reproduced with permission [67]. Copyright 2023, IEEE. (l) Multi-segment continuum magnetizable tentacle. Reproduced with permission [69]. Copyright 2020, IEEE.

PDMS and two permanent magnets (Figure 2b) [49]. Through a mathematical model, the relationship between the magnetic force and the deformation of the robot was described. This relationship was modeled by finite element analysis due to its nonlinearity. Experimentally, robot's deformation angles reaching up to 132.7° was achieved. Both two-dimensional (2D) and 3D tracking experiments demonstrated reliable manipulation performance. Furthermore, Lin et al. introduced a MCR that incorporates opposite-magnetized magnets. It designed to enhance dexterity through active multi-mode deformation, without compromising miniaturization by increasing structural complexity (Figure 2c) [50]. This MCR has the ability to multi deform, for example, C-, S- and J-shapes, to pass through different lumens of the body. To characterize the deformation of MCR, a mathematical model that integrated with the point-dipole field model and energy-based kinematics was developed.

To improve the operational capability of CRs, researchers combined phase change materials with MCRs. Mao et al. proposed a millimeter-scale continuum robot with 'follow-the-leader' behavior that achieves apical extension and structural stability (Figure 2d) [51]. Utilizing a dual-component system based on phase transitions, the robot underwent periodic, tip-based elongation guided by a programmable magnetic field. This allows for active programming and reprogramming of the robot's shape through trajectory planning of its tip, independent of environmental interactions. A cooperative MCR was also introduced, which achieved non-interactive navigation by utilizing low melting point alloy (LMPA) and implementing an alternating support strategy [52]. The CR accomplished independent multi-degree-of-freedom control of three magnetic units through the precise manipulation of phase changes in different segments. This allows for the versatile manipulator to be reconfigured in situ, enabling the completion of complex tasks.

The design of a concentric tube CR further improves the maneuverability of MCRs [53, 54]. Li et al. introduced the design and modeling of a homocentric variable-stiffness magnetic robotic catheter (Figure 2e) [55]. This continuum robotic system performs percutaneous coronary interventions procedures with the assistance of multi-robot control and ultrasound imaging. A hierarchical control framework is presented, encompassing multi-arm mobile permanent magnets, visual/force-serving-based mobile in-plane ultrasound tracking, and autonomous catheter navigation. The collaborative motion of the external mobile magnetic module and the extracorporeal mobile ultrasound module is regulated through the application of relative Jacobian-based control. The investigators validated the superior navigational performance of this MCR by performing preoperative planning in arteries for different scenarios.

Magnetic endoscopes, manipulated by an external controllable magnetic field, can reduce the difficulty of operating the system and patient discomfort. Pittiglio et al. discussed a novel control technique for capsule levitation in magnetically driven capsule colonoscopy [56]. Furthermore, Martin et al. demonstrated intelligent and autonomous control of magnetic flexible endoscope and the development of intelligent and autonomous control strategies makes a reduction in exertion for the user (Figure 2f) [57].

2.2 | MCR Integrated With Magnetic Matter

MCRs integrated with magnetic matter, such as magnetic particles, offer significant advantages in terms of flexibility, adaptability, and programmable magnetization direction [58–65]. Unlike rigid magnets, magnetic matter-based MCRs exhibit high flexibility to adapt to complex environments, enabling flexible navigation manipulation in confined lumens.

Kim et al. proposed a magnetic soft continuum robot (MSCR), which was composed of a homogeneous continuum of a soft polymer matrix with uniformly dispersed ferromagnetic microparticles (Figure 2g) [34]. To reduce the friction of the MSCR, hydrogel skin is grown on its surface. The magnetic material and soft, lubricated body give the robot excellent navigation performance. Bioprinting as a promising technology has been combined with MCRs in order to reduce the trauma of biological tissues. Zhou et al. introduced a ferromagnetic soft catheter robot system that enables in situ, computer-controlled bioprinting in a minimally invasive manner through magnetic actuation (Figure 2h) [66]. The soft catheter robot's design incorporates ferromagnetic particles dispersed within a fiber-reinforced polymer matrix, ensuring stable ink extrusion and accommodating a wide range of materials with varying rheological properties and functionalities. By utilizing a superimposed magnetic field, the MCR achieves digitally controlled printing.

One of the advantages of magnetic particles as components of the MCR is that programmable magnetization directions can be achieved. Zhang et al. proposed a magnetic guidewire, which is composed of a commercial guidewire with hydrophilic coating [35]. The basic material of magnetic continuum robot is Ecoflex and NdFeB microparticles, the mixed material can be programmed for the direction of magnetization of the magnetic tip by predeformation and magnetization (Figure 2i). To increase the magnetization strength of an MCR and design the desired magnetic profile. Wang et al. introduced an evolutionary design strategy to maximize the workspace of MSCR. It integrated theoretical modeling and genetic algorithm to identify the optimal magnetization and rigidity patterns of MSCR (Figure 2j) [68]. To address the challenge of functionalizing magnetic robots due to their low force output, a magnetic variable stiffness coiling robot was designed by utilizing Ecoflex and NdFeB microparticle combined with nitinol wires (Figure 2k) [67]. Lloyd et al. used a neural network training design method based on finite element analysis, by which the magnetization profile can be tailored to the specific anatomical constraints in order to achieve a design trajectory (Figure 2l) [69].

2.3 | MCR Integrated With Ferromagnetic Sphere

MCRs integrated with ferromagnetic spheres offer unique advantages in precision steering and flexible manipulation, especially in environments that require real-time localization and controlled navigation. The ferromagnetic sphere tip reaches saturation magnetization in the strong magnetic field of the MRI scanner. A magnetic force is subsequently applied to the ferromagnetic sphere tip through an external magnetic field gradient, which is aligned with the direction of the magnetic gradient. The magnetic force guided the MCRs for selective vascular catheter

insertion. Zhang et al. developed an intravascular catheter equipped with a ferromagnetic spherical tip designed for navigation using MRI gradient forces (Figure 3a) [36]. The ferromagnetic tip, with a diameter of 2 mm, is connected to the catheter via a flexible silicone tube, which minimizes friction with the vascular walls while maintaining sufficient flexibility for maneuvering. This innovative design enhances navigation accuracy and operational feasibility in an MRI environment, providing a novel tool for minimally invasive endovascular interventions. Lalande et al. utilized a custom-designed magnetic guidewire featuring a 0.9 mm ferromagnetic bead attached to its tip (Figure 3b) [70]. The bead is magnetized to saturation within the MRI system's magnetic field, and its movement is controlled by forces generated through additional gradient coils. The guidewire, made from flexible materials, is capable of precise navigation within complex vascular networks. This design ensures high maneuverability and compatibility with MRI environments, enabling selective arterial catheterization in a radiation-free setting. Gosselin et al. systematically quantified the bending characteristics of magnetic catheters actuated by magnetic gradient coils in an MRI system through theoretical modeling and experimental investigation. It explored the performance of single- and multi-sphere tip designs, revealing that multi-sphere designs significantly enhance deflection amplitude but require balancing the nonlinear effects caused by dipole-dipole interactions (Figure 3c) [37]. Strategies were proposed to achieve precise navigation by optimizing gradient strength, direction, and ferromagnetic material distribution, while addressing imaging artifacts in MRI. Zhang et al. introduced a catheter with a 2 mm ferromagnetic sphere tip connected via a flexible silicone tube for enhanced steerability (Figure 3d) [71]. By using a dual-echo projection technique with orthogonal rephasing gradients, they achieved precise localization while minimizing background noise. Phantom and in vivo tests demonstrated localization errors of 1.6 and 4 mm, respectively, highlighting its potential for accurate, radiation-free navigation in MR-guided interventions.

2.4 | MCR Integrated With Micro Coil

MCRs integrated with micro coils enhance performance in MRI-guided navigation [38, 72]. The integration of micro coils enables

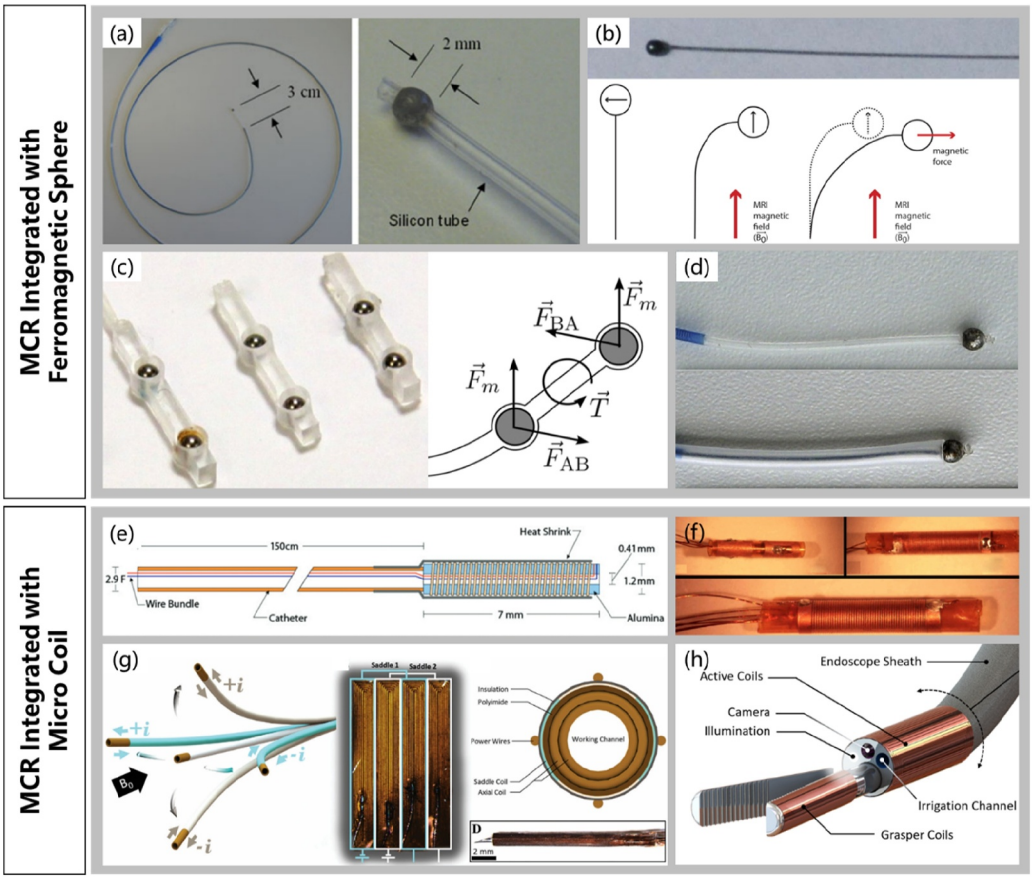

FIGURE 3 | MCR integrated with ferromagnetic sphere and micro coil. (a–d) MCRs integrated with ferromagnetic sphere: (a) Intravascular catheter with a ferromagnetic sphere. Reproduced with permission [36]. Copyright 2010, ESMRMB. (b) Magnetic guidewire with a ferromagnetic bead. Reproduced with permission [70]. Copyright 2015, American Association of Physicists in Medicine. (c) Magnetic catheter tips with two magnetic spheres. Reproduced with permission [37]. Copyright 2011, American Association of Physicists in Medicine. (d) Catheter connected to a 2 mm ferromagnetic sphere tip. Reproduced with permission [71]. Copyright 2013, Elsevier. (e–h) MCRs integrated with micro coil: (e) Magnetic catheter tip connected to a solenoid coil. Reproduced with permission [38]. Copyright 2014, RSNA. (f) Three-axis coil system assembled with a microcatheter. Reproduced with permission [73]. Copyright 2013, Elsevier. (g) Magnetic microcatheter with a quad-configuration micro coil. Reproduced with permission [39]. Copyright 2022, The Authors. (h) Endoscopic system with grasping and remote steering coils. Reproduced with permission [74]. Copyright 2022, IEEE.

current-dependent magnetization, allowing for efficient control of the CRs' movement through the application of external magnetic fields. Unlike traditional magnetic components, micro coils can be tuned to generate specific magnetic force and torque, enabling fine-tuned steering and real-time imaging with minimal artifacts. Losey et al. presented a magnetically controlled catheter with a 2 mm solenoid coil at the tip for precise steering under MRI guidance (Figure 3e) [38]. The design uses foot pedal-controlled currents for tip deflection, achieving higher success rates and shorter procedure times compared to manual guidance. Wilson et al. introduced the development of a magnetically controlled catheter designed for precise navigation under magnetic resonance imaging guidance [73]. The catheter integrates orthogonal coils, fabricated through laser lithography, at its 2 mm tip to enable controlled multi-directional deflection (Figure 3f). By applying varying currents to the coils, the catheter achieves predictable and precise steering, verified through phantom studies. Phelan et al. proposed a magnetically controlled catheter equipped with a quad-configuration micro coil system, enabling precise Lorentz force-based steering under magnetic resonance imaging guidance (Figure 3g) [39]. The catheter, with a 1 mm diameter design, optimizes power efficiency and minimizes heating risks while achieving tip deflections up to 110° with a 4-degree error margin. Using innovative laser-fabricated coils, the design reduces tip weight and bulk, enhancing navigation in confined anatomical spaces such as neurovascular and renal systems. To improve the application of MCRs, Phelan et al. proposed a system integrates Lorentz force-based steering mechanisms with an optimized design featuring axial and quad micro coils at the endoscope tip (Figure 3h) [74]. This enables precise and controllable bending up to 90° while mitigating heat generation, addressing a critical challenge in MRI-compatible devices. Furthermore, the inclusion of a grasping mechanism capable of applying forces up to 31 mN facilitates both soft tissue manipulation and tumor ablation with low power inputs. These innovations underscore the potential of combining real-time MRI guidance with advanced steering and ablation capabilities to enhance precision, safety, and efficacy in minimally invasive neurointerventions.

3 | Actuation and Manipulation of MCR

This section explains the actuation and control strategies of MCR. First, the theory behind magnetic actuation of MCR will be introduced, including different modeling approaches for MCR. Subsequently, different magnetic actuation platforms used in various systems will be discussed. Then various control strategies and corresponding MCR's autonomous level employed are presented.

3.1 | Actuation Theory of MCR

Since MCR is a type of long slender object belonging to continuum robot, the classic methods could be applied to modeling of it. Many modeling strategies have been developed to predict the kinematics of MCRs, which can be divided into the following three examples: cosserat rod theory, constant curvature assumption, and rigid-link model (Figure 4). These different methods coincide with MCR actuation methods, which describe the outcome of equilibrium between internal and external magnetic forces and torques.

1. Cosserat rod theory

Cosserat rod theory is widely used for the static equilibrium of continuum robot without simplifying assumptions. Regarding MCR, this method consists of solving a set of equilibrium equations between the position, orientation, internal force, and internal torque of the robot, providing high consistency and accuracy for modeling bending, torsion, and extension under magnetic actuations [46, 75–78]. However, cosserat rod theory involves solving complex nonlinear partial differential equations requiring numerical and time-consuming calculations, which presents challenges and complexity in controlling tip of MCR. Moreover, the theory may struggle to model certain behaviors like large rotations or significant twisting deformations without additional modifications.

2. Constant curvature assumption

Constant curvature assumption is based on the assumption that each segment of the continuum robot deforms in a constant radius arc. In other words, the curvature keeps invariant along the lengths. Compared with cosserat rod theory, it simplifies the computation cost and numerical intensity of the continuum robot's shape and motion when modeling [43, 79–82]. Also, piece-wise constant curvature defines the robot is modeled as a series of links that can deflect with constant curvature. Although this approach is widely used, when facing large

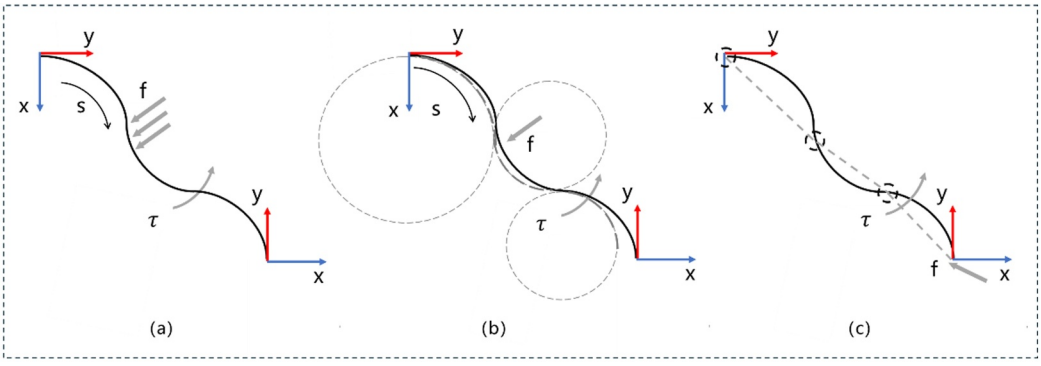

FIGURE 4 | Schematic diagram of three classical modeling approaches for continuum robots. (a) Cosserat rod theory. (b) Constant curvature assumption. (c) Rigid-link model. f and τ illustrate the vector fields force and torque with respect to the robot's length s, respectively.

bending and twisting in multiple directions, it will lead to inaccuracy and complexity in the predicted shape of CR.

3. Rigid-link model

The rigid-link model is a simplification commonly used to model continuum robots or robotic manipulators. In this approach, the robot can be divided into small enough segments which are represented as a series of connected rigid links [83–87]. Each link is assumed to be inflexible, however, causing impractical behaviors or numerous variables [88].

In addition to the classical methods mentioned above, finite element methods (FEM) have been widely used to analyze the deformation properties of MCRs and for experimental validation. Through FEM, the deformation of MCRs under magnetic interaction can be accurately calculated in a simulation environment [49, 89, 90]. However, the calculation of complex deformation of MCRs by the finite element method may consume more computational resources and time, and the calculation time can be significantly reduced by comparing and selecting the appropriate modeling method through the study [64, 65]. To balance the modeling accuracy and computational efficiency of MCRs, some kinds of new modeling approaches for continuum robot were further studied and utilized: such as neural network training methods, and other more affine-to-control modeling approaches [69, 91]. To achieve real-time control of MCR, researchers should investigate more accurate modeling methods with minimization of computational burden.

3.2 | Magnetic Actuation Platform

Magnetic actuation platforms have been systematically summarized in [92, 93]. In this section, the main focus is on some of the permanent magnetic and electromagnetic actuation platforms used and potentially available for actuating MCR.

1. Actuation magnetic field analysis

The external actuation magnetic field of MCR is typically generated by either permanent magnet or electromagnet. This section provides a concise overview of the analytical approaches and computational methods for evaluating both permanent magnetic fields and electromagnetic fields in spatial contexts. In the equations below, boldface type denotes a vector and regular type denotes a scalar.

In an idealized scenario, treating the magnetic source as a magnetic dipole $\boldsymbol{m}$ located at a point $\boldsymbol{P_m}$ in space, the magnetic field $\boldsymbol{b}$ at a point $\boldsymbol{P_b}$ is given by Equation (1) and the corresponding field distribution generated by the magnetic dipole is illustrated in Figure 5a [94].

$$\boldsymbol{b}\{\boldsymbol{P_b}, \boldsymbol{m}, \boldsymbol{P_m}\} = \left(\frac{\mu_0}{4\pi\|\boldsymbol{P_b} - \boldsymbol{P_m}\|^5}\left(3(\boldsymbol{P_b} - \boldsymbol{P_m})(\boldsymbol{P_b} - \boldsymbol{P_m})^{\mathrm{T}} - \|\boldsymbol{P_b} - \boldsymbol{P_m}\|^2 \mathbb{I}_3\right)\right)\boldsymbol{m} \tag{1}$$

where $\mu_0 = 4\pi \times 10^{-7}\ \mathrm{T{\cdot}m{\cdot}A^{-1}}$ is the permeability of free space, $\mathbb{I}_3$ is a 3×3 identity matrix. It can also be represented as an alternative form given by Equation (2).

$$\boldsymbol{b}\{\boldsymbol{r}, \boldsymbol{m}\} = \left(\frac{\mu_0}{4\pi\|\boldsymbol{r}\|^3}\left(3\hat{\boldsymbol{r}}\hat{\boldsymbol{r}}\mathrm{T} - \mathbb{I}_3\right)\right)\boldsymbol{m} \tag{2}$$

where $\boldsymbol{r} = \boldsymbol{P_b} - \boldsymbol{P_m}$. In non-idealized scenario, however, the magnetic source cannot be regarded as a point. Therefore, a multipole expansion is performed

$$\boldsymbol{b}\{\boldsymbol{r}, \boldsymbol{m}\} = \left(\frac{\mu_0}{4\pi\|\boldsymbol{r}\|^3}\mathbb{P}_1\hat{\boldsymbol{r}} + \frac{\mu_0}{4\pi\|\boldsymbol{r}\|^5}\mathbb{P}_2\hat{\boldsymbol{r}} + \frac{\mu_0}{4\pi\|\boldsymbol{r}\|^7}\mathbb{P}_3\hat{\boldsymbol{r}} + \ldots\right)\boldsymbol{m} \tag{3}$$

which is possible to accurately approximate the value of the magnetic field $\boldsymbol{b}$ at $\boldsymbol{P_b}$ with respect to the center-of-mass position $\boldsymbol{P_m}$. In the expansion terms it can be noted that the first term decays with $\|\boldsymbol{r}\|^{-3}$, the second with $\|\boldsymbol{r}\|^{-5}$, the third with $\|\boldsymbol{r}\|^{-7}$, and so on. $\mathbb{P}$ matrices in Equation (3) are shape functions that are independent of the distance from the magnetic source. Furthermore, the accuracy of the dipole model will increase as the distance from the source increases.

To determine the magnetic field $\boldsymbol{b}$ at a point $\boldsymbol{P_b}$ resulting from an electric current i passing through a wire coil, the Biot–Savart law

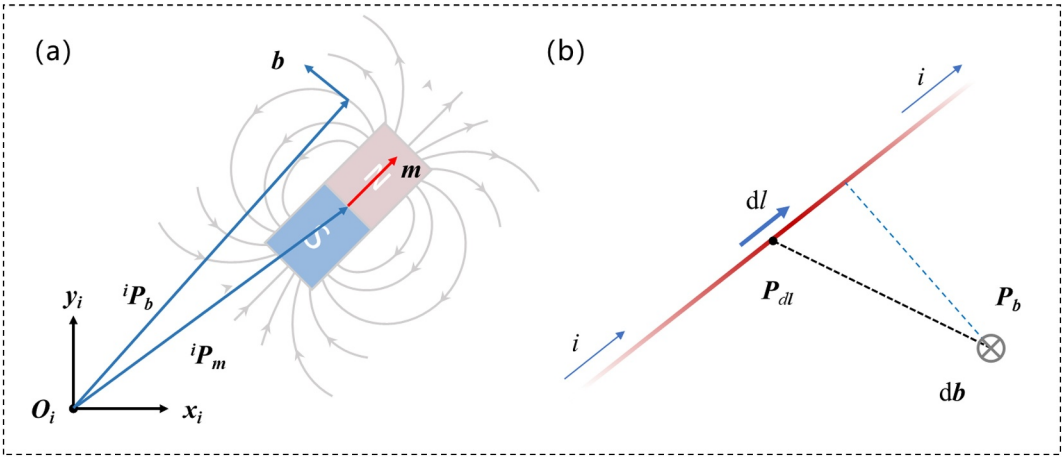

FIGURE 5 | Magnetic field illustration. (a) Magnetic field of a permanent magnet as a magnetic dipole. (b) An electric current element $id\boldsymbol{l}$ through a wire produces a magnetic field $d\boldsymbol{b}$ at point $\boldsymbol{P_b}$.

is applied (Figure 5b). This law begins by considering a small segment of the conductor with length d$\boldsymbol{l}$ positioned at a point $\boldsymbol{P}_{dl}$. The contribution to the magnetic field from this tiny segment is d$\boldsymbol{b}$, and by integrating the contributions from every infinitesimal segment along the conductor, we obtain the total magnetic field at $\boldsymbol{P}_{\boldsymbol{b}}$, which is given by Equation (4):

$$\begin{aligned}\boldsymbol{b}\{\boldsymbol{P}_{\boldsymbol{b}}, i\} &= \int d\boldsymbol{b} = \int \mu_0 \frac{i d\boldsymbol{l} \times (\boldsymbol{P}_{\boldsymbol{b}} - \boldsymbol{P}_{dl})}{4\pi \|\boldsymbol{P}_{\boldsymbol{b}} - \boldsymbol{P}_{dl}\|^3} \\ &= \frac{\mu_0 i}{4\pi} \int \frac{\mathbb{S}\{\boldsymbol{P}_{dl} - \boldsymbol{P}_{\boldsymbol{b}}\}}{\|\boldsymbol{P}_{\boldsymbol{b}} - \boldsymbol{P}_{dl}\|^3} d\boldsymbol{l}\end{aligned} \tag{4}$$

where $\mathbb{S}\{\text{vector}\}$ is the skew-symmetric matrix representation of a vector used in the cross-product operation. When the straight wires form a circular loop, a magnetic field distribution similar to that in Figure 5a is produced. This magnetic field $\boldsymbol{m}$ can be described by a multipole expansion, and its dipole moment can be calculated using Equation (5):

$$\boldsymbol{m}\{i\} = \frac{i}{2} \int \mathbb{S}\{\boldsymbol{P}_{dl} - \boldsymbol{P}_r\} d\boldsymbol{l} \tag{5}$$

where $\boldsymbol{P}_r$ is an arbitrary fixed reference point. It can be seen that the dipole moment of the coil is linearly related to the current. For a circular loop of thin wire with radius r, the dipole moment is $\boldsymbol{m} = \pi r^2 i \hat{\boldsymbol{a}}$, with $\hat{\boldsymbol{a}}$ being the direction of the area vector, which can be expressed by the right-hand rule. For a cylindrical coil with inner radius r_i and thickness t, the dipole moment can be calculated as $\boldsymbol{m} = \pi\left(r_i^2 + r_i t + \frac{1}{3}t^2\right) i \hat{\boldsymbol{a}}$.

2. Permanent magnetic actuation platform

Permanent magnets offer several advantages as magnetic field sources for actuating magnetic robots [95–98]. They generate stable and persistent magnetic fields without requiring external power. Their simple structure and ease of integration reduce system complexity. Integrating a permanent magnet with a robotic arm as a magnetic actuation system expands the operating space of the permanent magnet as a magnetic source [98–100].

Wright et al. developed a spherical-actuator-magnet manipulator designed for magnetic manipulation using a single spherical permanent magnet [101]. The system features a spherical permanent magnet driven by three orthogonal omniwheels, enabling holonomic, singularity-free control of the magnet's dipole orientation (Figure 6a). Magnetic field sensors provide real-time feedback, enabling closed-loop control through a Kalman filter-based estimation system. Pittiglio et al. investigated a novel magnetic actuation system for soft-tethered capsule colonoscopy using a single external permanent magnet manipulated by a robotic arm (Figure 6b) [56]. The system's efficacy was validated through experiments in both controlled and realistic environments, demonstrating significantly reduced contact with the colon wall and improved traversal efficiency compared to conventional methods. Yang et al. proposed a dual-mode magnetic actuation platform designed for intravascular ultrasound imaging, utilizing an external permanent magnet for actuation without a conventional drive shaft (Figure 6c) [102]. It features an acoustic-magnetic tip integrating a radially magnetized permanent magnet and an ultrasound transducer, enabling both active steering and shaft-free ultrasound beam scanning. A robotic arm adjusts the magnet's position and orientation to generate static magnetic fields for navigation and dynamic fields for imaging. Li et al. introduced an external magnetic actuation platform consisting of a cylindrical permanent magnet mounted on the end-effector of a six-degree-of-freedom robotic arm (Figure 6d) [55]. A hierarchical control strategy coordinates the robotic arm's movements using a relative Jacobian-based framework. This enables synchronized magnetic catheter manipulation, ultrasound-guided tracking, and force feedback control.

The configuration of multiple permanent magnets provides a way to design a magnetic actuation system. Zhou et al. designed an external magnetic control platform including four motor-driven permanent magnets arranged symmetrically (Figure 6e) [66]. By adjusting the magnets' positions and orientations, the system generates a non-uniform magnetic field, inducing forces and torques that enable the catheter's bending, rotation, and translation. A numerical control strategy correlates magnet displacements with catheter tip movements, ensuring accurate, remote-controlled bioprinting along complex 3D surfaces. To enable independent control of parallel continuum soft magnetic manipulators in a shared confined environment, Koszowska et al. utilized a magnetic control approach, employing a magnetic actuation platform with dual robotic control over external permanent magnets (Figure 6f) [103]. This platform facilitates the decoupled control of magnetic force and torque, accomplished through the manipulation of linear gradients and homogeneous fields, respectively [100].

3. Electromagnetic actuation platform

Electromagnetic actuation systems offer key advantages for driving magnetic robots due to their controllability and adaptability. They provide dynamically adjustable magnetic fields through electric current modulation, enabling precise control of robot movement, force, and orientation. This tunability supports complex motion patterns, including feedback-driven and real-time responses. Through an electromagnetic actuation platform, flexible steering and magnetic manipulation of MCR can be achieved [104–109]. Electromagnetic systems can generate both uniform and gradient fields, facilitating diverse tasks such as targeted manipulation, trajectory planning, and autonomous navigation for magnetic microrobots [110–115].

The ARMM system is an advanced magnetic actuation platform designed for precise control of flexible surgical instruments, featuring a mobile electromagnetic coil mounted on a six-degree-of-freedom robotic arm (Figure 6g) [41]. The system's design optimizes magnetic field generation while balancing payload and thermal constraints through a systematic optimization process. A real-time iterative map-based control strategy compensates for core saturation and field non-linearities by adjusting the coil's position and current using feedback from Hall-effect sensors. This enables accurate force and torque generation for steering instruments in a large, scalable workspace. With its ability to perform precise, responsive, and adaptive actuation, the ARMM system holds significant potential for minimally invasive surgical procedures requiring complex navigation and manipulation.

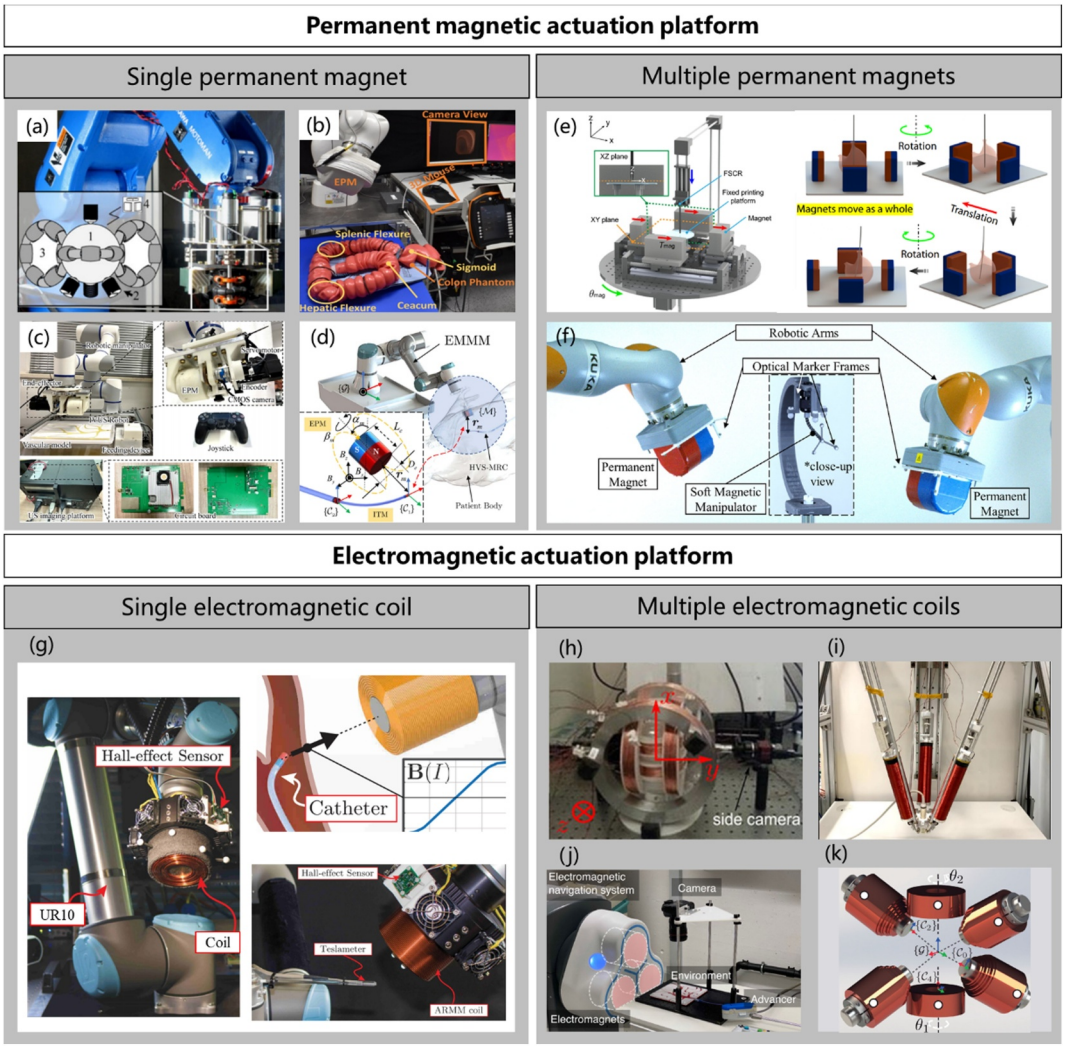

FIGURE 6 | Magnetic actuation platforms. (a–f) Permanent magnetic actuation platforms: (a) SAMM system consisting of a spherical magnet, three omni-wheels, and a robotic arm. Reproduced with permission [101]. Copyright 2017, IEEE. (b) Magnetic actuation platform consisting of an external magnet and a robotic arm. Reproduced with permission [56]. Copyright 2019, IEEE. (c) Dual-mode magnetic actuation platform consisting of a permanent magnet, a servo motor, and a robotic arm. Reproduced with permission [102]. Copyright 2025, IEEE. (d) External mobile magnetic module consisting of a cylindrical permanent magnet fixed on the 6 DOF robotic arm. Reproduced with permission [55]. Copyright 2024, IEEE. (e) Magnetic actuation platform consisting of four mobile permanent magnets. Reproduced with permission [66]. Copyright 2021, The Authors. (f) Dual external permanent magnet platform. Reproduced with permission [103]. Copyright 2023, The Authors. (g–k) Electromagnetic actuation platforms: (g) ARMM system comprises 6 DOF mobile electromagnet. Reproduced with permission [41]. Copyright 2019, IEEE. (h) Helmholtz coil. Reproduced with permission [116]. Copyright 2015, IEEE. (i) Electromagnetic actuation platform with three electromagnets. Reproduced with permission [43]. Copyright 2021, IEEE. (j) Electromagnetic navigation platform consisting of three parallel coils with triangle arrangement. Reproduced with permission [117]. Copyright 2022, IEEE. (k) BigMag: magnetic actuation platform consisting of six mobile coils array. Reproduced with permission [118]. Copyright 2019, IEEE.

The design featuring multiple electromagnets improves the maneuverability of the magnetic actuation system, but also increases its complexity. Helmholtz coils, a widely utilized electromagnetic actuation system, are employed in actuating magnetic robots due to their capability to generate a highly uniform magnetic field within the central region of the coil configuration (Figure 6h) [116]. Moreover, in order to magnetically actuate the MCR while realizing imaging guidance, an electromagnetic actuation platform combining three parallel electromagnets and an ultrasound probe was developed [43]. Dreyfus et al. introduced a novel simulation framework for MCRs, which illustrated the magnetic actuation and interactions forces with meshed collision models [117]. The simulator was evaluated using an electromagnetic actuation platform composed of 3 parallel coils (Figure 6j). BigMag, a high bandwidth magnetic actuation platform comprised of six electromagnetic coils, was employed for accurate actuation of MCR [118]. The configuration of the electromagnetic actuation platform is depicted in Figure 6k.

4. MRI-based magnetic actuation system

In addition to laboratory-developed permanent magnetic actuation platforms and electromagnetic actuation platforms, commercially available MRI systems have been used as a type of magnetic-actuation system. MRI enables sub-millimeter-

resolution soft-tissue imaging while providing high magnetic-field gradients, enabling the actuation, localization, and control of MCRs for interventional manipulation. MCRs integrated ferromagnetic spheres or micro coils in Section 2.3 and 2.4 are navigated under MRI system. Azizi et al. introduced fringe field navigation (FFN), which used high-gradient fringe fields from clinical MRI scanner [119]. It guided MCR into narrow blood vessels by magnetic pulling forces. Traditional methods rely on the scanner's main magnetic field. FFN instead exploits the gradients of MRI's outer fringe fields. This approach addressed reduced guidewire stiffness hinders steerability in narrow vessels. In order to be more adaptable to clinical scenarios, Tiryaki et al. proposed MCRs' actuation at ultrahigh magnetic fields (UHF) in MRI scanners [120]. They found that magnets can maintain nonparallel magnetization relative to the MRI's main field, enabling unique actuation opportunities. The team conducted obstacle avoidance and vascular navigation tasks in 2D and 3D environments, showcasing the guidewire's ability to navigate complex structures.

MRI systems integrate high-precision imaging and actuation in MCRs' manipulation. Compared with CT and x-ray imaging modalities, MRI is free of ionizing radiation, which reduces the health risks for doctors and patients. Combining the diagnostic imaging of MRI with the positioning and control of MCRs can improve the precision and safety of interventional procedures [121]. However, the problem of sequences between imaging and actuation of MRI systems may affect the driving smoothness and control accuracy of MCRs. The operating space is limited by the aperture of the MRI scanner and the system is expensive.

3.3 | Control Strategy of MCR

The control system of MCRs consists of different actuation blocks and control strategies which can be divided into four layers according to their autonomous level [122–124]. Each layer represents specialized robotic operation of MCRs, characterizing with increasing autonomy, reflecting the significant improvement in the level of control strategies for MCRs with the sophistication of the magnetic platform and the intelligence of the control algorithms.

The most utilized and simplest layer is defined as 'manual operation'. In this layer, users manipulate MCRs via controlling a permanent magnet manually. As shown in Figure 7a,b, researchers use the gradient force of permanent magnets and attraction to MCRs to deflect and navigate by manually adjusting its angle and distance [33, 34, 50, 125]. This manual control can be associated with level 0, since the driving and movement of MCRs are dependent on the experience and feeling of the manipulator, lacking a certain degree of control effectiveness, accuracy and experimental safety.

In the second layer (level 1), users control MCRs to accomplish a defined task through pre-input system parameters such as magnet position, input electromagnetic coil current, end-effector trajectory, etc [30, 89, 126–128]. To achieve MCRs parametric operation, researchers established several kinds of magnetic platforms. An example shows that Mao et al. introduced a magnetic steering continuum robot under eight-electromagnetic coil system, which can be programmed the deformation of its tip through trajectory planning [51]. Zhou et al. designed a four-permanent-magnet magnetic field printing system to realize trajectory control of the end of MCR by pre-inputting the magnetic field position and trajectory parameters to satisfy the requirements of open surgery for printing on internal organs (Figure 7d) [66]. However, in this autonomous level, MCRs are controlled indirectly by tuning different magnetic field parameters, this control strategy cannot be able to balance real-time control stability and manipulation accuracy. In addition, this control mode of MCRs is inefficient and does not directly model the motion of the tip of MCRs.

The next layer with medium autonomy is called 'robotic operation', which enables users to focus on and control the position and orientation of MCRs directly [129]. It requires a more complex control system with more advanced algorithms such as tracking, localization, and pose estimation. In this layer, human operators only need to focus on controlling MCRs based on the image feedback of surrounding environments. The relevant required magnetic field parameters will be calculated and generated automatically. In most cases, operators utilized joystick and 3-dimensional mouse to control MCRs for delivering and navigation. Kim et al. introduced a telerobotic neurointerventional platform with a joystick controller with a 6 DOF knob to control the robot end effector for spatial positioning of the magnet remotely (Figure 7e) [130]. Dreyfus et al. operated a highly dexterous, magnetically steered continuum robot via joystick demonstrated through successful navigation in models of the human vasculature and in blood vessels of a live pig (Figure 7f) [32]. Besides, many MCRs robotic systems were developed with different remote control strategies. In this control layer, researchers have applied different control algorithms for MCRs' steering and motion. In [46], a visual-feedback controller was developed to steer the permanent magnetic component-based catheters using the specially designed electromagnetic coil system. In [131], a double-Loop stable control method for magnetic guidewire steering was developed aiming to avoid vessel damage.

In the fourth layer, the control level can be associated to level 3 which is called 'semi-autonomous robotic operation'. With the increasing of autonomy, the navigation task of MCRs is performed autonomously, transferring the decision priority to the system. Compared with level 2 Robotic operation, the semi-autonomous robotic operation involves more advanced control frameworks and strategies and focus on the improving the autonomy of control system. In this level, such as deep reinforcement learning (DRL)-based methods are widely utilized for the actuation system to guide MCRs with high precision. Moreover, in level 3, Autonomous decision-making awareness and environmental adaptability of MCRs are improved, as the system can manipulate them to make different decisions in the face of different complex environments in order to efficiently accomplish the given task at this level.

In most cases, system will generate control strategies such as changing magnetic field position, rotation, and orientation but under supervision of the operator, who can perform discrete control actions and override the autonomous control to select a different output for MCRs. As shown in Figure 7g, researchers used machine vision to develop intelligent and autonomous

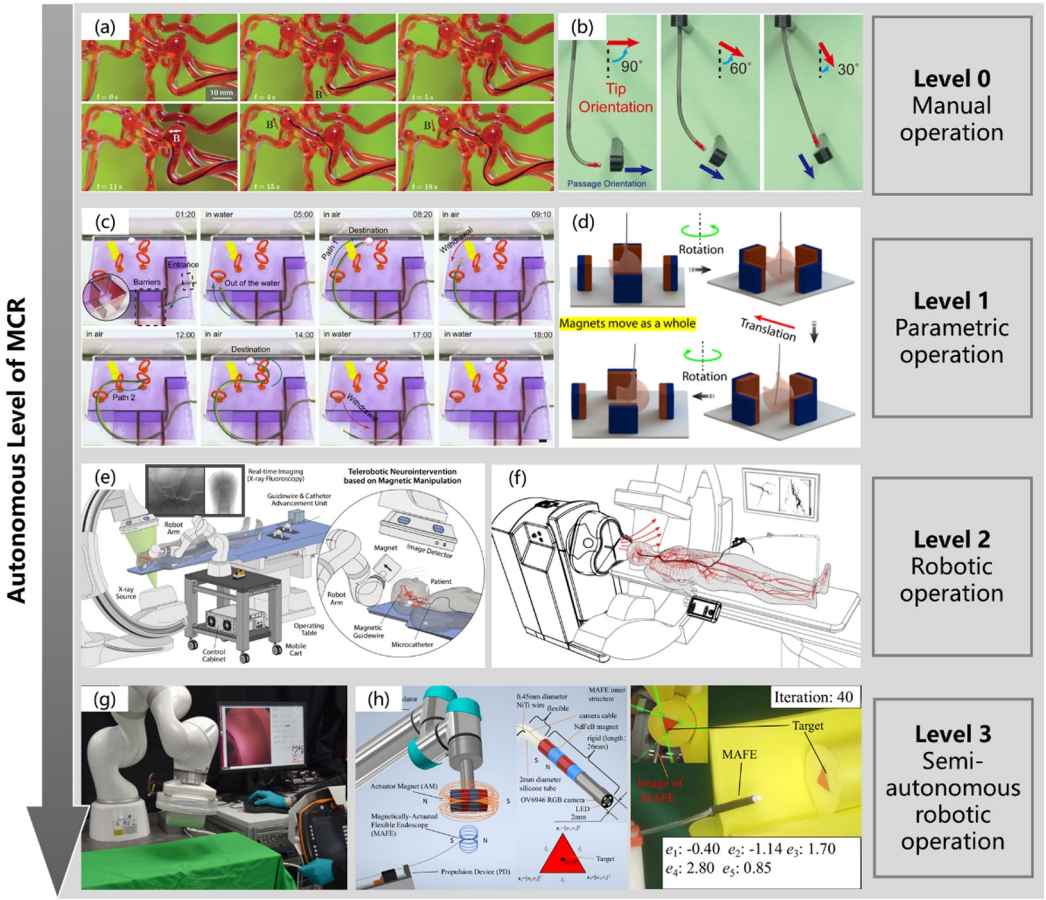

FIGURE 7 | Autonomous level of MCR. (a) Ferromagnetic soft continuum robot. Reproduced with permission [34]. Copyright 2019, AAAS. (b) Opposite-polarized MCR. Reproduced with permission [33]. Copyright 2023, IEEE. (c) Programmable shape and functionalities MCR. Reproduced with permission [51]. Copyright 2024, The Authors. (d) Ferromagnetic soft catheter robot for bioprinting. Reproduced with permission [66]. Copyright 2021, The Authors. (e) MCR for telerobotic neurovascular intervention. Reproduced with permission [130]. Copyright 2022, AAAS. (f) Helical MCR for endovascular navigation. Reproduced with permission [32]. Copyright 2024, AAAS. (g) Magnetic endoscope with intelligent and autonomous manipulation. Reproduced with permission [57]. Copyright 2020, Springer Nature. (h) Magnetic flexible endoscope with model-free and uncalibrated visual-feedback control. Reproduced with permission [132]. Copyright 2022, IEEE.

control of a magnetic flexible endoscope, enabling non-expert users to perform magnetic colonoscopy in vivo effectively [57]. In [132], Tan et al. proposed algorithms to enhance the pose control of magnetically actuated flexible endoscopes and experiments in structured environments verified that the control algorithms could realize 4 DOF manual navigation and 5 DOF autonomous navigation (Figure 7h).

In the discussion of levels of autonomy, the control of MCRs is getting more automatic and intelligent, from manual operation to navigation by changing systematic parameters, then to direct control algorithms on MCRs, and the final level is generating adaptive actions for completing delivery tasks. After introducing the increasing autonomy level of controlling MCRs, the next section summarizes and focuses on the different types of operational tasks performed by MCRs using intelligent manipulation.

4 | Manipulation Tasks of MCR

Depending on the design principles and structural configurations, a diverse range of manipulative tasks can be accomplished by MCRs through advanced control strategies. This section aims to explore the various manipulation capabilities of MCRs, explaining how these manipulations are achieved by magnetic fields in real-world applications. By examining the interplay between design, control, and magnetic actuation, this section highlights the versatility and potential of MCRs in performing complex manipulation tasks.

4.1 | Navigation

Navigation, a fundamental operation of the MCR, is intrinsically linked to the system's overall performance and efficiency. Enhanced precision and intelligent navigation capabilities enable the MCR to maneuver through more intricate and constrained environments, thereby laying the essential groundwork for the successful execution of other advanced manipulations. The ability to navigate with high accuracy and adaptability is a critical determinant of the MCR's versatility and functional scope across a variety of applications.

The MCR in [32] overcomes the propulsion limitations of conventional devices by converting rotational motion into forward motion through helical protrusions on its surface that contact the

vessel wall (Figure 8a). At the same time, its segmentally articulated magnetic tip design improves the maneuverability and flexibility of magnetic navigation, allowing it to successfully navigate to the brain's tiny arteries. The navigation task of the MCR is remotely controlled by the operator at the dedicated console, with visual feedback via x-ray images during navigation. The advancement and rotation of the MCR were accomplished by the advancer unit, while the active deflection of magnetic tip was achieved by the electromagnetic navigation system. A method which utilized a rotating magnetic field to assist MSCR in navigating through a narrow and tortuous lumen was proposed [133]. By combining mechanical insertion and the dynamic remodeling force generated by the rotating magnetic field, the MSCR is able to smoothly advance through the soft lumen in a serpentine motion, effectively reducing

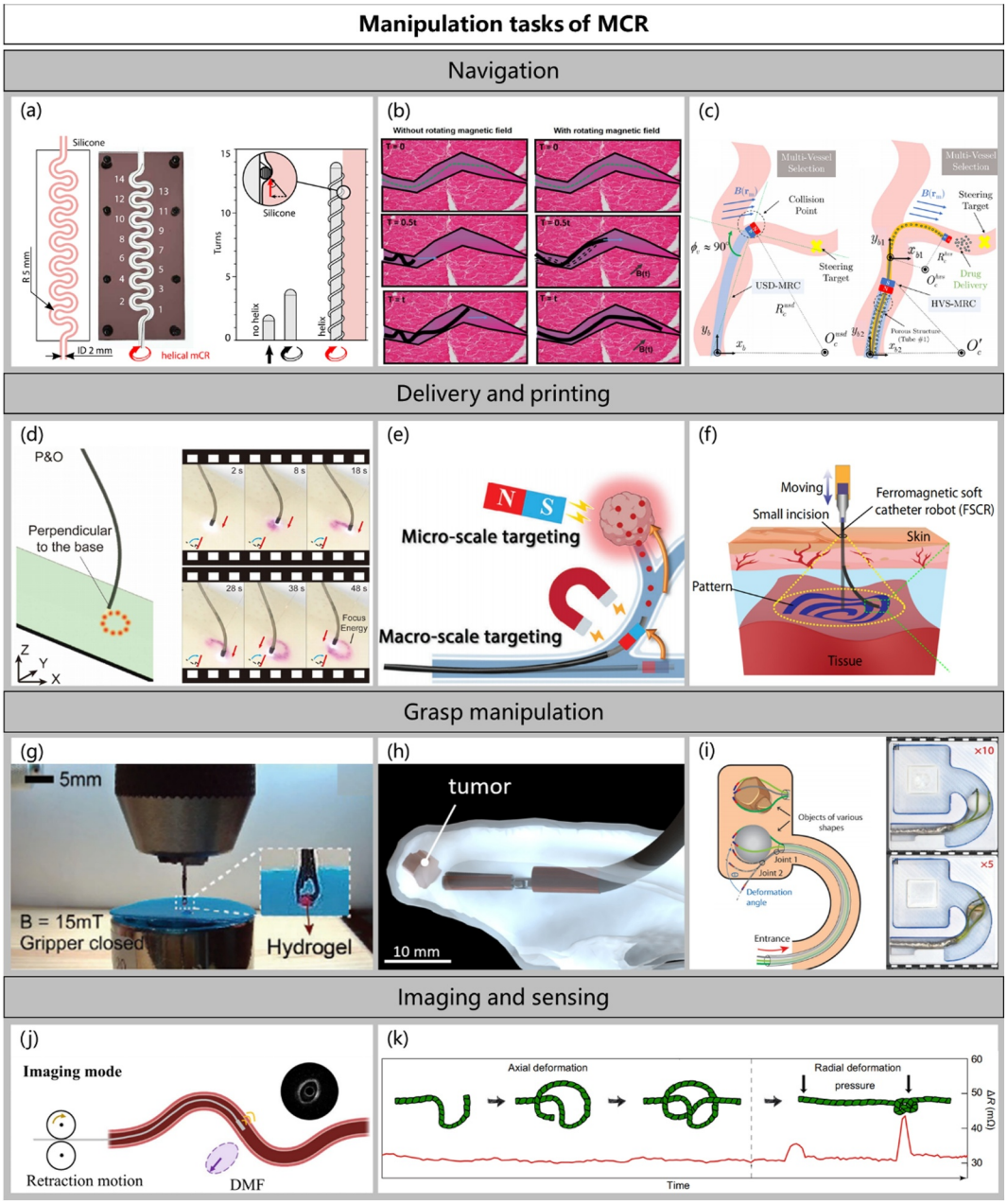

FIGURE 8 | Manipulation tasks of MCR. (a) Helical MCR navigating in the flat vessel model. Reproduced with permission [32]. Copyright 2024, AAAS. (b) MSCR navigating in pancreatic duct with/without rotating external magnetic field. Reproduced with permission [133]. Copyright 2024, IEEE. (c) Homocentric MCR navigating in the multivessel selection. Reproduced with permission [55]. Copyright 2024, IEEE. (d) MCR embedded with a violet LED to simulate the laser manipulation. Reproduced with permission [33]. Copyright 2023, IEEE. (e) MCR for cross-scale targeted drug delivery. Reproduced with permission [134]. Copyright 2023, Wiley-VCH. (f) Ferromagnetic soft catheter robot for in situ printing. Reproduced with permission [66]. Copyright 2021, The Authors. (g) Hydrogel grasp manipulation of MCR. Reproduced with permission [135]. Copyright 2023, Wiley-VCH. (h) Tumor grasp manipulation of MCR. Reproduced with permission [74]. Copyright 2022, IEEE. (i) Objects of various shapes manipulation of MCR. Reproduced with permission [52]. Copyright 2024, Wiley-VCH. (j) Intravascular ultrasound imaging through MCR. Reproduced with permission [102]. Copyright 2025, IEEE. (k) MCR tying itself into a knot to sense radial pressure. Reproduced with permission [51]. Copyright 2024, The Authors.

the insertion force and avoiding buckling. The insertion manipulation was accomplished by a linear actuator and the rotating magnetic field was generated by two rotating permanent magnets. Experimental results show that this method can significantly reduce the required insertion force by about 45% and triple the insertion depth in a fixed time, while enabling the MSCR to traverse channels smaller than its diameter (Figure 8b). The variable stiffness characteristic can improve MCR's navigation capability in variable lumen environments. The MCR achieves variable stiffness through the telescopic motion of the concentric-containing components, and is able to adapt to complex coronary environments actuated by external magnetic field (Figure 8c) [55]. Combining a hierarchical control strategy with preoperative planning, the MCR enables navigation through different segments in the arterial phantom.

4.2 | Delivery and Printing

MCRs for delivery, which are employed to move drugs to the target area, while printing, similar to additive manufacturing, leverages the robot's dexterity for intricate and customized trajectory planning.

A laser surgery simulation was demonstrated, which using MCR equipped with integrated LED [33]. By precisely controlling the position and orientation of the MCR tip, which was maintained perpendicular to the flat plate, ensuring focused light energy and producing a uniform illumination spot (Figure 8d). A marsupial robotic system was proposed that leverages a miniature MCR and chemical/magnetic hybrid nanorobots for intracranial cross-scale targeted drug delivery in glioblastoma therapy [134]. The MCR, with its small dimensions, flexible body, and programmable active motion, enables macroscale targeting by transporting the nanorobots through a minimally invasive channel to the brain (Figure 8e). A ferromagnetic soft catheter robot (FSCR) system enables the printing of functional inks with different rheological properties on flat and curved surfaces through magnetic actuation [66]. The experiment involved printing conductive hydrogels onto porcine tissue phantoms and the surface of a rat liver in vivo through minimally invasive incisions (Figure 8f).

4.3 | Grasp Manipulation

Grasp manipulation in MCR is achieved through their unique structural design and suitable control strategies. The flexible, continuum structure of the MCR enables shape transformation, while magnetic force control provides remote manipulation capabilities. This synergy allows the robot to securely capture and stabilize objects by adjusting its configuration based on object properties. Such capabilities are crucial in applications such as robotic-assisted surgery, where delicate and deformable tissues require precise handling, and where both accuracy and adaptability are important.

Fan et al. introduced a magnetic fiber robot equipped with a micro-manipulation tool at its distal end [135]. Through magnetic field manipulation, the micro-gripper at the fiber end switches between open and closed states, allowing for the controlled grasping and release of objects (Figure 8g). Phelan et al. used a novel grasping mechanism integrated into an MRI-driven neuroendoscope, leveraging the principles of Lorentz force (Figure 8h) [74]. The grasping manipulation relies on micro coils that, when energized, generate a magnetic moment directly proportional to the current and coil area, causing a torque that bends the grasper to engage with tissue. Yang et al. introduced a multifunctional MCR equipped with advanced grasping capabilities [52]. The grasp manipulation is enabled by the extension of multiple CR individuals from the guider component. Each individual can independently bend and adapt to different shapes, allowing the robot to reconfigure into multifunctional manipulators such as multi-degree-of-freedom grippers at the target location. By controlling the heating current and programmable magnetic field, the robot can grasp objects with complex morphologies stably (Figure 8i).

4.4 | Imaging and Sensing

Imaging and sensing refer to MCRs' ability to integrate sensing technologies for capturing environmental data and interacting with their surroundings. This includes visual imaging and pressure sensing, enabling MCRs to perform real-time environmental monitoring and adjust their behavior accordingly.

Yang et al. developed a soft catheter with an acoustic-magnetic tip, which enables controllable bending under static magnetic fields for navigating complex vascular structures and shaft-free acoustic beam scanning under dynamic magnetic fields for high-resolution ultrasound imaging (Figure 8j) [102]. Furthermore, a novel motor-free telerobotic endomicroscopy system, which leverages mono-magnet actuation to enable steerable and programmable optical coherence tomography (OCT) imaging in complex and curved lumens [136]. In addition to imaging, force sensing is also realized through MCR [137]. A versatile MCR achieves pressure sensing by transforming its three-dimensional structure [51]. This adaptive capability is especially useful in open environments such as the stomach or bladder, where the robot can reshape into complex 3D configurations. A notable function is its ability to serve as a pressure sensor by forming tight knots, which significantly increase its sensitivity to radial deformation (Figure 8k). This structural adaptation enables precise detection of external factors such as intestinal pressure, enhancing its sensing performance in dynamic biological environments.

5 | Discussion

Research on MCRs has provided new diagnostic and therapeutic tools for medical applications. Thanks to the flexible body and dexterous manipulation of the distal end of MCRs, the risks involved in interventional procedures can be greatly reduced and the precision and safety of interventions can be improved. Many MCRs have been validated in theoretical and laboratory environments, but to ensure their effectiveness in real biological environments, they must be verified by interaction experiments with biological tissues. The influence of biological tissues on the control precision, functionality and safety of MCRs cannot be ignored.

Many studies have been carried out to validate the experiments from in vitro to in vivo. An MCR capable of active propulsion and

deflection was experimentally validated in 2D and 3D phantoms [138]. Path selection in tortuous and complex blood vessels was accomplished by a self-designed magnetic continuum robotic system. With the assistance of imaging systems, an MCR for remote-controlled neurovascular intervention achieved clot retrieval thrombectomy and aneurysm coil embolization in cerebrovascular phantoms, and was experimentally validated for in vivo remote magnetic navigation in a porcine model [130]. Through the unique helical protrusion structure design, the interaction between the MCR and biological tissues can be utilized to achieve the conversion of MCR rotation into propulsive motion, reducing the probability of snagging and injury occurring in vascular interventions [32]. Navigation experiments of the MCR have been validated in the human placenta and porcine models.

MCRs have significant promise for medical applications, particularly in minimally invasive surgery. Biological experiments serve as a critical bridge in the translation of MCRs from laboratory to clinical practice. Both in vitro and in vivo experiments can effectively verify the accuracy, stability, and safety of MCRs, while providing the necessary feedback and direction of improvement for the application of these robots in the clinic. In addition, research on MCRs should pay close attention to interdisciplinary cooperation, thus improving the intelligence and safety of MCRs in medical applications.

6 | Conclusion and Outlook

The MCR, with its unique design, structure, and control strategies, shows extraordinary potential in the medical field. It embeds magnetic components, employs flexible materials, and incorporates advanced manufacturing methods to enhance maneuverability and functionality in confined spaces. Its actuation system, combining with magnetic actuation and robotic control, further achieves the MCR's larger work space and precision control. In terms of the imaging system, the MCR is closely integrated with imaging technologies to achieve precise localization and visualization of in vivo manipulations, significantly improving the accuracy and safety. Meanwhile, the integration of intelligent control algorithms and human-robot collaboration technology enables lower operating difficulty and higher work efficiency. The future focus may be fourfold, as shown in Figure 9.

Advanced design and structure: Future MCR designs will concentrate on material innovation and structural optimization, aiming to enhance their operational flexibility and durability. By incorporating high-strength, high-flexibility materials, such as advanced alloys and composites [139–142], these robots will maintain exceptional performance in complex and variable environments. Additionally, optimization of structural design will further improve the robots' response speed and operational precision. The integration of biomimetic design principles is expected to enable the robots to better simulate the natural forms and movement patterns of biological tissues, thereby demonstrating higher adaptability and safety in biomedical applications. Advancements in sensor technology can significantly enhance the environmental sensing capabilities of MCRs, enabling real-time feedback and precise control, thereby facilitating higher levels of adaptive performance and intelligent manipulation. The integration of multimodal sensors within MCRs allows for the accurate detection of biological tissue properties, thereby enabling in situ monitoring and minimizing the risk of tissue damage [5, 102, 136]. Advanced manufacturing techniques also play a key role in fabricating MCRs efficiently and precisely [59, 143–147].

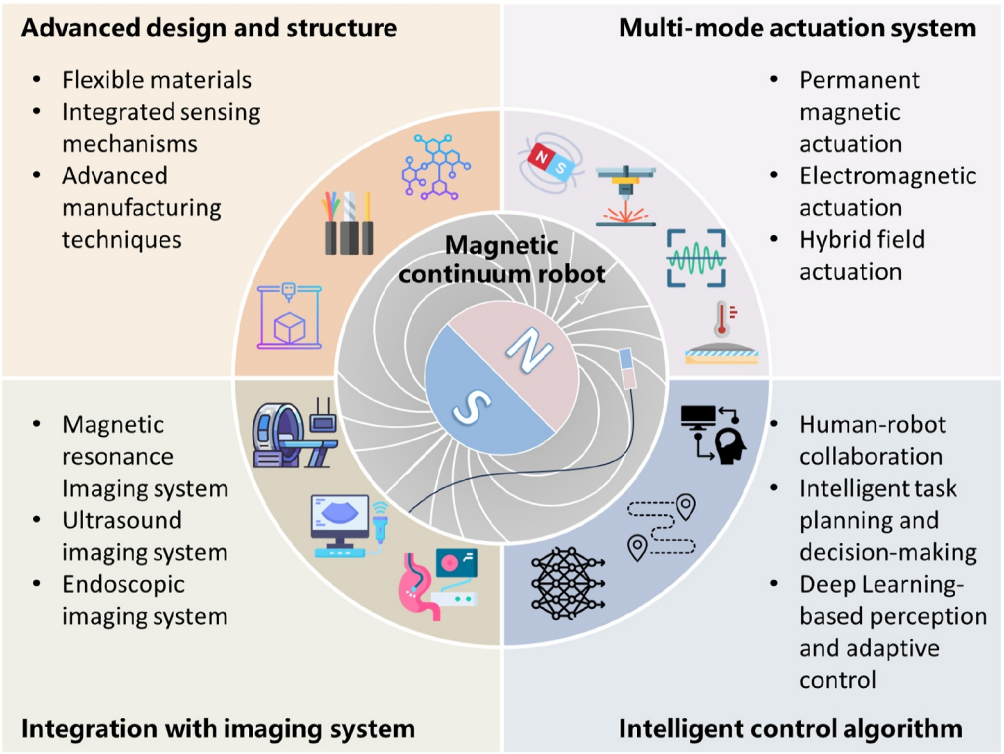

FIGURE 9 | Schematic diagram of future development priorities and directions for MCRs.

Multi-mode actuation system: In the future, MCRs will feature more intelligent and efficient multi-mode actuation systems. Magnetic actuation, electric actuation, optic actuation, and hybrid field actuation will ensure optimal performance of MCRs in different environments [148–151]. The introduction of intelligent algorithms will facilitate the stability of multi-actuation modes, significantly expanding MCRs' manipulation range and precision. Furthermore, the development of novel multi-mode actuation systems will endow MCRs with enhanced adaptability and operational flexibility in complex environments, further broadening their application potential across the medical field.

Integration of imaging system: The integration of imaging systems represents a crucial direction in the development of magnetic continuum robot technology. Through deep integration of techniques such as magnetic resonance imaging, ultrasound imaging, and endoscopic imaging, MCRs will be able to obtain real-time internal structural information, enabling precise detection and visualization of operational processes [152–158]. Simultaneously, the imaging systems will be closely combined with intelligent control algorithms to provide the robots with more comprehensive and accurate environmental information, thereby substantially improving the accuracy and safety of operations. As imaging technologies continue to advance, MCRs will support higher-resolution and more precise tissue imaging, bringing revolutionary changes to medical surgery, detection, and exploration.

Intelligent control algorithm: Advanced control algorithms are the core driving force behind MCRs. In the future, with the rapid development of artificial intelligence technologies, intelligent control algorithms will become more complex and efficient, enabling more refined and autonomous operations [57]. The introduction of deep learning algorithms will allow MCRs to learn from vast amounts of actual operational data, continuously optimizing control strategies and operational methods. The application of reinforcement learning techniques will enable MCRs to possess stronger autonomous decision-making and adaptive control capabilities in dynamic environments. Furthermore, the development of trajectory planning and human-robot collaboration control algorithms will enhance the safety and efficiency of human-robot interaction [31, 129, 130], enabling the robots to demonstrate outstanding performance in intelligent manipulations.

Author Contributions

Yuanbiao Ma: writing – original draft, investigation, writing – review and editing. **Xuanyu An:** writing – original draft, investigation, writing – review and editing. **Qijun Yang:** writing – original draft, visualization, writing – review and editing. **Mingxue Cai:** writing – review and editing. **Zhiqiang Tang:** writing – review and editing. **Jinke Chang:** writing – review and editing. **Veronica Iacovacci:** writing – review and editing. **Tiantian Xu:** writing – review and editing, project administration. **Li Zhang:** project administration. **Qianqian Wang:** conceptualization, methodology, writing – review and editing, funding acquisition, project administration, supervision.

Acknowledgments

The authors thank the financial support from the National Natural Science Foundation of China (No. 52205590), the Natural Science Foundation of Jiangsu Province (No. BK20220834), the Start-up Research Fund of Southeast University (No. RF1028623098), the Taihu Lake Innovation Fund for the School of Future Technology of Southeast University, and in part by SIAT-CUHK Joint Laboratory of Robotics and Intelligent Systems. Funded by the European Union. Views and opinions expressed are however those of the authors only and do not necessarily reflect those of the European Union or the European Research Council Executive Agency. Neither the European Union nor the granting authority can be held responsible for them. This work is supported by ERC grant (I-BOT, 101162939). Part of the elements in Figures 1 and 9 is created with Freepik.com.

Conflicts of Interest

The authors declare no conflicts of interest.

References

1. M. Russo, S. M. H. Sadati, X. Dong, et al., "Continuum Robots: An Overview," *Advanced Intelligent Systems* 5, no. 5 (2023): 2200367, https://doi.org/10.1002/aisy.202200367.

2. J. Burgner-Kahrs, D. C. Rucker, and H. Choset, "Continuum Robots for Medical Applications: A Survey," *IEEE Transactions on Robotics* 31, no. 6 (2015): 1261–1280, https://doi.org/10.1109/TRO.2015.2489500.

3. P. E. Dupont, N. Simaan, H. Choset, and C. Rucker, "Continuum Robots for Medical Interventions," *Proceedings of the IEEE* 110, no. 7 (2022): 847–870, https://doi.org/10.1109/JPROC.2022.3141338.

4. F. Alambeigi, S. Aghajani Pedram, J. L. Speyer, et al., "SCADE: Simultaneous Sensor Calibration and Deformation Estimation of FBG-Equipped Unmodeled Continuum Manipulators," *IEEE Transactions on Robotics* 36, no. 1 (2020): 222–239, https://doi.org/10.1109/TRO.2019.2946726.

5. C. Shi, X. Luo, P. Qi, et al., "Shape Sensing Techniques for Continuum Robots in Minimally Invasive Surgery: A Survey," *IEEE Transactions on Biomedical Engineering* 64, no. 8 (2017): 1665–1678, https://doi.org/10.1109/TBME.2016.2622361.

6. H. Alfalahi, F. Renda, and C. Stefanini, "Concentric Tube Robots for Minimally Invasive Surgery: Current Applications and Future Opportunities," *IEEE Transactions on Medical Robotics and Bionics* 2, no. 3 (2020): 410–424, https://doi.org/10.1109/TMRB.2020.3000899.

7. Z. Mitros, S. M. H. Sadati, R. Henry, L. Da Cruz, and C. Bergeles, "From Theoretical Work to Clinical Translation: Progress in Concentric Tube Robots," *Annual Review of Control, Robotics, and Autonomous Systems* 5, no. 1 (2022): 335–359, https://doi.org/10.1146/annurev-control-042920-014147.

8. D. Haraguchi, T. Kanno, K. Tadano, and K. Kawashima, "A Pneumatically Driven Surgical Manipulator With a Flexible Distal Joint Capable of Force Sensing," *IEEE* 20, no. 6 (2015): 2950–2961, https://doi.org/10.1109/TMECH.2015.2415838.

9. Z. Xie, F. Yuan, J. Liu, et al., "Octopus-inspired Sensorized Soft Arm for Environmental Interaction," *Science Robotics* 8, no. 84 (2023): eadh7852, https://doi.org/10.1126/scirobotics.adh7852.

10. K. Ikuta, Y. Matsuda, D. Yajima, and Y. Ota, "Pressure Pulse Drive: A Control Method for the Precise Bending of Hydraulic Active Catheters," *IEEE* 17, no. 5 (2012): 876–883, https://doi.org/10.1109/TMECH.2011.2138711.

11. Y. Bailly, Y. Amirat, and G. Fried, "Modeling and Control of a Continuum Style Microrobot for Endovascular Surgery," *IEEE Transactions*

on Robotics 27, no. 5 (2011): 1024–1030, https://doi.org/10.1109/TRO.2011.2151350.

12. L. Pancaldi, P. Dirix, A. Fanelli, et al., "Flow Driven Robotic Navigation of Microengineered Endovascular Probes," *Nature Communications* 11, no. 1 (2020): 6356, https://doi.org/10.1038/s41467-020-20195-z.

13. T. Gopesh, J. H. Wen, D. Santiago-Dieppa, et al., "Soft Robotic Steerable Microcatheter for the Endovascular Treatment of Cerebral Disorders," *Science Robotics* 6, no. 57 (2021): eabf0601, https://doi.org/10.1126/scirobotics.abf0601.

14. K. Oliver-Butler, J. A. Childs, A. Daniel, and D. C. Rucker, "Concentric Push–Pull Robots: Planar Modeling and Design," *IEEE Transactions on Robotics* 38, no. 2 (2022): 1186–1200, https://doi.org/10.1109/TRO.2021.3104249.

15. W. Lai, L. Cao, R. X. Tan, et al., "Force Sensing With 1 mm Fiber Bragg Gratings for Flexible Endoscopic Surgical Robots," *IEEE* 25, no. 1 (2020): 371–382, https://doi.org/10.1109/TMECH.2019.2951540.

16. M. S. Moses, R. J. Murphy, M. D. M. Kutzer, and M. Armand, "Modeling Cable and Guide Channel Interaction in a High-Strength Cable-Driven Continuum Manipulator," *IEEE* 20, no. 6 (2015): 2876–2889, https://doi.org/10.1109/TMECH.2015.2396894.

17. H. Xie, M. Sun, X. Fan, et al., "Reconfigurable Magnetic Microrobot Swarm: Multimode Transformation, Locomotion, and Manipulation," *Science Robotics* 4, no. 28 (2019): eaav8006, https://doi.org/10.1126/scirobotics.aav8006.

18. Q. Wang, N. Xiang, J. Lang, B. Wang, D. Jin, and L. Zhang, "Reconfigurable Liquid-Bodied Miniature Machines: Magnetic Control and Microrobotic Applications," *Advanced Intelligent Systems* 6, no. 2 (2024): 2300108, https://doi.org/10.1002/aisy.202300108.

19. V. Iacovacci, E. Diller, D. Ahmed, and A. Menciassi, "Medical Microrobots," *Annual Review of Biomedical Engineering* 26, no. 1 (2024): 561–591, https://doi.org/10.1146/annurev-bioeng-081523-033131.

20. M. Cao, R. Sheng, Y. Sun, et al., "Delivering Microrobots in the Musculoskeletal System," *Nano-Micro Letters* 16, no. 1 (2024): 251, https://doi.org/10.1007/s40820-024-01464-8.

21. Q. Wang, S. Yang, and L. Zhang, "Untethered Micro/Nanorobots for Remote Sensing: Toward Intelligent Platform," *Nano-Micro Letters* 16, no. 1 (2024): 40, https://doi.org/10.1007/s40820-023-01261-9.

22. Q. Wang, K. F. Chan, K. Schweizer, et al., "Ultrasound Doppler-Guided Real-Time Navigation of a Magnetic Microswarm for Active Endovascular Delivery," *Science Advances* 7, no. 9 (2021): eabe5914, https://doi.org/10.1126/sciadv.abe5914.

23. B. Wang, K. F. Chan, K. Yuan, et al., "Endoscopy-assisted Magnetic Navigation of Biohybrid Soft Microrobots With Rapid Endoluminal Delivery and Imaging," *Science Robotics* 6, no. 52 (2021): eabd2813, https://doi.org/10.1126/scirobotics.abd2813.

24. B. Wang, Q. Wang, K. F. Chan, et al., "tPA-Anchored Nanorobots for In Vivo Arterial Recanalization at Submillimeter-Scale Segments," *Science Advances* 10, no. 5 (2024): eadk8970, https://doi.org/10.1126/sciadv.adk8970.

25. Q. Wang, Z. Ning, K. F. Chan, et al., "Tracking and Navigation of a Microswarm Under Laser Speckle Contrast Imaging for Targeted Delivery," *Science Robotics* 9, no. 87 (2024): eadh1978, https://doi.org/10.1126/scirobotics.adh1978.

26. X. Du and J. Yu, "Image-Integrated Magnetic Actuation Systems for Localization and Remote Actuation of Medical Miniature Robots: A Survey," *IEEE Transactions on Robotics* 39, no. 4 (2023): 2549–2568, https://doi.org/10.1109/TRO.2023.3271582.

27. P. R. Slawinski, A. Z. Taddese, K. B. Musto, K. L. Obstein, and P. Valdastri, "Autonomous Retroflexion of a Magnetic Flexible Endoscope," *IEEE Robotics and Automation Letters* 2, no. 3 (2017): 1352–1359, https://doi.org/10.1109/LRA.2017.2668459.

28. T. L. Bruns, K. E. Riojas, D. S. Ropella, et al., "Magnetically Steered Robotic Insertion of Cochlear-Implant Electrode Arrays: System Integration and First-In-Cadaver Results," *IEEE Robotics and Automation Letters* 5, no. 2 (2020): 2240–2247, https://doi.org/10.1109/LRA.2020.2970978.

29. S. L. Charreyron, Q. Boehler, A. N. Danun, A. Mesot, M. Becker, and B. J. Nelson, "A Magnetically Navigated Microcannula for Subretinal Injections," *IEEE Transactions on Biomedical Engineering* 68, no. 1 (2021): 119–129, https://doi.org/10.1109/TBME.2020.2996013.

30. P. Lloyd, O. Onaizah, G. Pittiglio, D. K. Vithanage, J. H. Chandler, and P. Valdastri, "Magnetic Soft Continuum Robots With Braided Reinforcement," *IEEE Robotics and Automation Letters* 7, no. 4 (2022): 9770–9777, https://doi.org/10.1109/LRA.2022.3191552.

31. G. Pittiglio, P. Lloyd, T. da Veiga, et al., "Patient-Specific Magnetic Catheters for Atraumatic Autonomous Endoscopy," *Soft Robotics* 9, no. 6 (2022): 1120–1133, https://doi.org/10.1089/soro.2021.0090.

32. R. Dreyfus, Q. Boehler, S. Lyttle, et al., "Dexterous Helical Magnetic Robot for Improved Endovascular Access," *Science Robotics* 9, no. 87 (2024): eadh0298, https://doi.org/10.1126/scirobotics.adh0298.

33. D. Lin, W. Chen, K. He, N. Jiao, Z. Wang, and L. Liu, "Position and Orientation Control of Multisection Magnetic Soft Microcatheters," *IEEE* 28, no. 2 (2023): 907–918, https://doi.org/10.1109/TMECH.2022.3213934.

34. Y. Kim, G. A. Parada, S. Liu, and X. Zhao, "Ferromagnetic Soft Continuum Robots," *Science Robotics* 4, no. 33 (2019): eaax7329, https://doi.org/10.1126/scirobotics.aax7329.

35. S. Zhang, M. Yin, Z. Lai, et al., "Design and Characteristics of 3D Magnetically Steerable Guidewire System for Minimally Invasive Surgery," *IEEE Robotics and Automation Letters* 7, no. 2 (2022): 4040–4046, https://doi.org/10.1109/LRA.2022.3146909.

36. K. Zhang, A. J. Krafft, R. Umathum, F. Maier, W. Semmler, and M. Bock, "Real-time MR Navigation and Localization of an Intravascular Catheter With Ferromagnetic Components," *Magn. Reson. Mater. Phys. Biol. Med.* 23, no. 3 (2010): 153–163, https://doi.org/10.1007/s10334-010-0214-y.

37. F. P. Gosselin, V. Lalande, and S. Martel, "Characterization of the Deflections of a Catheter Steered Using a Magnetic Resonance Imaging System," *Medical Physics* 38, no. 9 (2011): 4994–5002, https://doi.org/10.1118/1.3622599.

38. A. D. Losey, P. Lillaney, A. J. Martin, et al., "Magnetically Assisted Remote-Controlled Endovascular Catheter for Interventional MR Imaging: In Vitro Navigation at 1.5 T versus X-Ray Fluoroscopy," *Radiology* 271, no. 3 (2014): 862–869, https://doi.org/10.1148/radiol.14132041.

39. M. F. Phelan, M. E. Tiryaki, J. Lazovic, H. Gilbert, and M. Sitti, "Heat-Mitigated Design and Lorentz Force-Based Steering of an MRI-Driven Microcatheter toward Minimally Invasive Surgery," *Advanced Science* 9, no. 10 (2022): 2105352, https://doi.org/10.1002/advs.202105352.

40. J. Sikorski, A. Denasi, G. Bucchi, S. Scheggi, and S. Misra, "Vision-Based 3-D Control of Magnetically Actuated Catheter Using BigMag—An Array of Mobile Electromagnetic Coils," *IEEE* 24, no. 2 (2019): 505–516, https://doi.org/10.1109/TMECH.2019.2893166.

41. J. Sikorski, C. M. Heunis, F. Franco, and S. Misra, "The ARMM System: An Optimized Mobile Electromagnetic Coil for Non-linear Actuation of Flexible Surgical Instruments," *IEEE Transactions on Magnetics* 55, no. 9 (2019): 1–9, https://doi.org/10.1109/TMAG.2019.2917370.

42. C. Chautems, A. Tonazzini, Q. Boehler, S. H. Jeong, D. Floreano, and B. J. Nelson, "Magnetic Continuum Device With Variable Stiffness for Minimally Invasive Surgery," *Advanced Intelligent Systems* 2, no. 6 (2020): 1900086, https://doi.org/10.1002/aisy.201900086.

43. Z. Yang, L. Yang, M. Zhang, Q. Wang, C. H. Simon, and L. Zhang, "Magnetic Control of a Steerable Guidewire Under Ultrasound

Guidance Using Mobile Electromagnets," *IEEE Robotics and Automation Letters* 6, no. 2 (2021): 1280–1287, https://doi.org/10.1109/LRA.2021.3057295.

44. D. Lin, J. Wang, N. Jiao, Z. Wang, and L. Liu, "A Flexible Magnetically Controlled Continuum Robot Steering in the Enlarged Effective Workspace With Constraints for Retrograde Intrarenal Surgery," *Advanced Intelligent Systems* 3, no. 10 (2021): 2000211, https://doi.org/10.1002/aisy.202000211.

45. V. N. T. Le, N. H. Nguyen, K. Alameh, R. Weerasooriya, and P. Pratten, "Accurate Modeling and Positioning of a Magnetically Controlled Catheter Tip," *Medical Physics* 43, no. 2 (2016): 650–663, https://doi.org/10.1118/1.4939228.

46. J. Edelmann, A. J. Petruska, and B. J. Nelson, "Magnetic Control of Continuum Devices," *International Journal of Robotics Research* 36, no. 1 (2017): 68–85, https://doi.org/10.1177/0278364916683443.

47. Y. Cao, Z. Yang, B. Hao, et al., "Magnetic Continuum Robot With Intraoperative Magnetic Moment Programming," *Soft Robotics* 10, no. 6 (2023): 1209–1223, https://doi.org/10.1089/soro.2022.0202.

48. D. Lin, N. Li, N. Jiao, Z. Wang, and L. Liu, "Kinematic Analysis of Multi-Section Opposite Magnetic Catheter Robots With Solution Multiplicity," *IEEE Transactions on Automation Science and Engineering* 21, no. 1 (2024): 123–134, https://doi.org/10.1109/TASE.2022.3229416.

49. S. Jeon, A. K. Hoshiar, K. Kim, et al., "A Magnetically Controlled Soft Microrobot Steering a Guidewire in a Three-Dimensional Phantom Vascular Network," *Soft Robotics* 6, no. 1 (2019): 54–68, https://doi.org/10.1089/soro.2018.0019.

50. D. Lin, N. Jiao, Z. Wang, and L. Liu, "A Magnetic Continuum Robot With Multi-Mode Control Using Opposite-Magnetized Magnets," *IEEE Robotics and Automation Letters* 6, no. 2 (2021): 2485–2492, https://doi.org/10.1109/LRA.2021.3061376.

51. L. Mao, P. Yang, C. Tian, et al., "Magnetic Steering Continuum Robot for Transluminal Procedures With Programmable Shape and Functionalities," *Nature Communications* 15, no. 1 (2024): 3759, https://doi.org/10.1038/s41467-024-48058-x.

52. P. Yang, L. Mao, C. Tian, X. Meng, and H. Xie, "A Cooperative and Multifunctional Magnetic Continuum Robot for Noninteractive Access, Dexterous Navigation, and Versatile Manipulation," *Advanced Functional Materials* 35, no. 2 (2024): 2412543, https://doi.org/10.1002/adfm.202412543.

53. Q. Peyron, Q. Boehler, P. Rougeot, et al., "Magnetic Concentric Tube Robots: Introduction and Analysis," *International Journal of Robotics Research* 41, no. 4 (2022): 418–440, https://doi.org/10.1177/02783649211071113.

54. Z. Li and Q. Xu, "Multi-Section Magnetic Soft Robot With Multi-robot Navigation System for Vasculature Intervention," *Cyborg and Bionic Systems* 5 (2024): 0188, https://doi.org/10.34133/cbsystems.0188.

55. Z. Li, J. Li, Z. Wu, Y. Chen, M. Yeerbulati, and Q. Xu, "Design and Hierarchical Control of a Homocentric Variable-Stiffness Magnetic Catheter for Multiarm Robotic Ultrasound-Assisted Coronary Intervention," *IEEE Transactions on Robotics* 40 (2024): 2306–2326, https://doi.org/10.1109/TRO.2024.3378442.

56. G. Pittiglio, L. Barducci, J. W. Martin, et al., "Magnetic Levitation for Soft-Tethered Capsule Colonoscopy Actuated With a Single Permanent Magnet: A Dynamic Control Approach," *IEEE Robotics and Automation Letters* 4, no. 2 (2019): 1224–1231, https://doi.org/10.1109/LRA.2019.2894907.

57. J. W. Martin, B. Scaglioni, J. C. Norton, et al., "Enabling the Future of Colonoscopy With Intelligent and Autonomous Magnetic Manipulation," *Nature Machine Intelligence* 2, no. 10 (2020): 595–606, https://doi.org/10.1038/s42256-020-00231-9.

58. Y. Ni, Y. Sun, H. Zhang, X. Li, S. Zhang, and M. Li, "Data-Driven Navigation of Ferromagnetic Soft Continuum Robots Based on Machine Learning," *Advanced Intelligent Systems* 5, no. 2 (2023): 2200167, https://doi.org/10.1002/aisy.202200167.

59. M. H. D. Ansari, V. Iacovacci, S. Pane, et al., "3D Printing of Small-Scale Soft Robots With Programmable Magnetization," *Advanced Functional Materials* 33, no. 15 (2023): 2211918, https://doi.org/10.1002/adfm.202211918.

60. K. Abolfathi, J. A. Rosales-Medina, H. Khaksar, et al., "Independent and Hybrid Magnetic Manipulation for Full Body Controlled Soft Continuum Robots," *IEEE Robotics and Automation Letters* 8, no. 7 (2023): 4235–4242, https://doi.org/10.1109/LRA.2023.3280749.

61. M. H. D. Ansari, X. T. Ha, M. Ourak, et al., "Characterization of a 3D Printed Endovascular Magnetic Catheter," *Actuators* 12, no. 11 (2023): 409, https://doi.org/10.3390/act12110409.

62. Y. Huang, Q. Zhao, J. Hu, and H. Liu, "Design and Modeling of a Multi-DoF Magnetic Continuum Robot With Diverse Deformation Modes," *IEEE Robotics and Automation Letters* 9, no. 4 (2024): 3956–3963, https://doi.org/10.1109/LRA.2024.3374192.

63. M. Brockdorff, T. da Veiga, J. Davy, et al., "Hybrid Trajectory Planning of Two Permanent Magnets for Medical Robotic Applications," *International Journal of Robotics Research* (2024): 02783649241264844, https://doi.org/10.1177/02783649241264844.

64. J. Li, H. Chen, and L. Wang, "Model-guided Navigation of Magnetic Soft Guidewire for Safe Endovascular Surgery," *Journal of the Mechanics and Physics of Solids* 190 (2024): 105731, https://doi.org/10.1016/j.jmps.2024.105731.

65. J. Li and L. Wang, "Modeling Magnetic Soft Continuum Robot in Nonuniform Magnetic Fields via Energy Minimization," *International Journal of Mechanical Sciences* 282 (2024): 109688, https://doi.org/10.1016/j.ijmecsci.2024.109688.

66. C. Zhou, Y. Yang, J. Wang, et al., "Ferromagnetic Soft Catheter Robots for Minimally Invasive Bioprinting," *Nature Communications* 12, no. 1 (2021): 5072, https://doi.org/10.1038/s41467-021-25386-w.

67. P. Lloyd, T. L. Thomas, V. K. Venkiteswaran, et al., "A Magnetically-Actuated Coiling Soft Robot With Variable Stiffness," *IEEE Robotics and Automation Letters* 8, no. 6 (2023): 3262–3269, https://doi.org/10.1109/LRA.2023.3264770.

68. L. Wang, D. Zheng, P. Harker, A. B. Patel, C. F. Guo, and X. Zhao, "Evolutionary Design of Magnetic Soft Continuum Robots," *Proceedings of the National Academy of Sciences* 118, no. 21 (2021): e2021922118, https://doi.org/10.1073/pnas.2021922118.

69. P. Lloyd, A. K. Hoshiar, T. da Veiga, et al., "A Learnt Approach for the Design of Magnetically Actuated Shape Forming Soft Tentacle Robots," *IEEE Robotics and Automation Letters* 5, no. 3 (2020): 3937–3944, https://doi.org/10.1109/LRA.2020.2983704.

70. V. Lalande, F. P. Gosselin, M. Vonthron, et al., "*In Vivo* Demonstration of Magnetic Guidewire Steerability in a MRI System With Additional Gradient Coils," *Medical Physics* 42, no. 2 (2015): 969–976, https://doi.org/10.1118/1.4906194.

71. K. Zhang, F. Maier, A. J. Krafft, R. Umathum, W. Semmler, and M. Bock, "Tracking of an Interventional Catheter With a Ferromagnetic Tip Using Dual-Echo Projections," *Journal of Magnetic Resonance* 234 (2013): 176–183, https://doi.org/10.1016/j.jmr.2013.06.020.

72. T. P. L. Roberts, W. V. Hassenzahl, S. W. Hetts, and R. L. Arenson, "Remote Control of Catheter Tip Deflection: An Opportunity for Interventional MRI," *Magnetic Resonance in Medicine* 48, no. 6 (2002): 1091–1095, https://doi.org/10.1002/mrm.10325.

73. M. W. Wilson, A. B. Martin, P. Lillaney, et al., "Magnetic Catheter Manipulation in the Interventional MR Imaging Environment," *Journal of Vascular and Interventional Radiology* 24, no. 6 (2013): 885–891, https://doi.org/10.1016/j.jvir.2013.01.487.

74. M. F. Phelan, N. O. Dogan, J. Lazovic, and M. Sitti, "Design and Development of a Lorentz Force-Based MRI-Driven Neuroendoscope," in

2022 IEEE/RSJ International Conference on Intelligent Robots and Systems (IROS) (IEEE, 2022), 9534–9541, https://doi.org/10.1109/IROS47612.2022.9981526

75. D. C. Rucker and R. J. Webster Iii, "Statics and Dynamics of Continuum Robots With General Tendon Routing and External Loading," *IEEE Transactions on Robotics* 27, no. 6 (2011): 1033–1044, https://doi.org/10.1109/TRO.2011.2160469.

76. I. Tunay, "Spatial Continuum Models of Rods Undergoing Large Deformation and Inflation," *IEEE Transactions on Robotics* 29, no. 2 (2013): 297–307, https://doi.org/10.1109/TRO.2012.2232532.

77. D. Trivedi, C. D. Rahn, W. M. Kier, and I. D. Walker, "Soft Robotics: Biological Inspiration, State of the Art, and Future Research," *Applied Bionics and Biomechanics* 5, no. 3 (2008): 99–117, https://doi.org/10.1080/11762320802557865.

78. J. Wang, J. Xue, S. Yuan, J. Tan, S. Song, and M. Q.-H. Meng, "Kinematic Modeling of Magnetically-Actuated Robotic Catheter in Nonlinearly-Coupled Multi-Field," *IEEE Robotics and Automation Letters* 6, no. 4 (2021): 8189–8196, https://doi.org/10.1109/LRA.2021.3104620.

79. H. Sun, J. Liu, and Q. Wang, "Design and Evaluation of Magnetic Navigation Flexible Endoscope for Colorectal Treatment," *IEEE Transactions on Applied Superconductivity* 32, no. 6 (2022): 1–5, https://doi.org/10.1109/TASC.2022.3167365.

80. R. J. Webster and B. A. Jones, "Design and Kinematic Modeling of Constant Curvature Continuum Robots: A Review," *International Journal of Robotics Research* 29, no. 13 (2010): 1661–1683, https://doi.org/10.1177/0278364910368147.

81. S. Song, H. Ge, J. Wang, and M. Q.-H. Meng, "Real-Time Multi-Object Magnetic Tracking for Multi-Arm Continuum Robots," *IEEE Transactions on Instrumentation and Measurement* 70 (2021): 1–9, https://doi.org/10.1109/TIM.2021.3124853.

82. T. Zhang, L. Yang, X. Yang, R. Tan, H. Lu, and Y. Shen, "Millimeter-Scale Soft Continuum Robots for Large-Angle and High-Precision Manipulation by Hybrid Actuation," *Advanced Intelligent Systems* 3, no. 2 (2021): 2000189, https://doi.org/10.1002/aisy.202000189.

83. R. J. Roesthuis and S. Misra, "Steering of Multisegment Continuum Manipulators Using Rigid-Link Modeling and FBG-Based Shape Sensing," *IEEE Transactions on Robotics* 32, no. 2 (2016): 372–382, https://doi.org/10.1109/TRO.2016.2527047.

84. V. K. Venkiteswaran, J. Sikorski, and S. Misra, "Shape and Contact Force Estimation of Continuum Manipulators Using Pseudo Rigid Body Models," *Mechanism and Machine Theory* 139 (2019): 34–45, https://doi.org/10.1016/j.mechmachtheory.2019.04.008.

85. J. Sikorski, C. M. Heunis, R. Obeid, V. K. Venkiteswaran, and S. Misra, "A Flexible Catheter System for Ultrasound-Guided Magnetic Projectile Delivery," *IEEE Transactions on Robotics* 38, no. 3 (2022): 1959–1972, https://doi.org/10.1109/TRO.2021.3123865.

86. M. M. R. S. Abadi, H. N. Pishkenari, and M. Yousefi, "Developing an Energy-Based Three-Dimensional Pseudo-rigid-body Model Founded on Kirchhoff Rod Theory for Magnetic Continuum Robots," in *2022 10th RSI International Conference On Robotics And Mechatronics (ICRoM), Tehran, Iran, Islamic Republic of* (IEEE, 2022), 42–47, https://doi.org/10.1109/ICRoM57054.2022.10025180.

87. P. Lloyd, G. Pittiglio, J. H. Chandler, and P. Valdastri, "Optimal Design of Soft Continuum Magnetic Robots Under Follow-The-Leader Shape Forming Actuation," in *2020 International Symposium on Medical Robotics (ISMR)* (IEEE, 2020), 111–117, https://doi.org/10.1109/ISMR48331.2020.9312943.

88. T. Da Veiga, J. H. Chandler, P. Lloyd, et al., "Challenges of Continuum Robots in Clinical Context: A Review," *Progress in Biomedical Engineering* 2, no. 3 (2020): 032003, https://doi.org/10.1088/2516-1091/ab9f41.

89. R. Zhao, Y. Kim, S. A. Chester, P. Sharma, and X. Zhao, "Mechanics of Hard-Magnetic Soft Materials," *Journal of the Mechanics and Physics of Solids* 124 (2019): 244–263, https://doi.org/10.1016/j.jmps.2018.10.008.

90. J. Park, H. Lee, H. Choi, et al., "Magnetically Steerable Asymmetric Magnetized Soft Continuum Robot (AMSCR) for Minimally Invasive Surgery," in *2022 International Conference on Robotics and Automation (ICRA)* (IEEE, 2022), 9586–9592, https://doi.org/10.1109/ICRA46639.2022.9811361.

91. C. Della Santina, A. Bicchi, and D. Rus, "On an Improved State Parametrization for Soft Robots With Piecewise Constant Curvature and its Use in Model Based Control," *IEEE Robotics and Automation Letters* 5, no. 2 (2020): 1001–1008, https://doi.org/10.1109/LRA.2020.2967269.

92. Z. Yang and L. Zhang, "Magnetic Actuation Systems for Miniature Robots: A Review," *Advanced Intelligent Systems* 2, no. 9 (2020): 2000082, https://doi.org/10.1002/aisy.202000082.

93. Y. Huo, L. Yang, T. Xu, and D. Sun, "Design, Control, and Clinical Applications of Magnetic Actuation Systems: Challenges and Opportunities," *Advanced Intelligent Systems* (2024): 2400403, https://doi.org/10.1002/aisy.202400403.

94. J. J. Abbott, E. Diller, and A. J. Petruska, "Magnetic Methods in Robotics," *Annual Review of Control, Robotics, and Autonomous Systems* 3, no. 1 (2020): 57–90, https://doi.org/10.1146/annurev-control-081219-082713.

95. W. Zhang, Y. Meng, and P. Huang, "A Novel Method of Arraying Permanent Magnets Circumferentially to Generate a Rotation Magnetic Field," *IEEE Transactions on Magnetics* 44, no. 10 (2008): 2367–2372, https://doi.org/10.1109/TMAG.2008.2002505.

96. M. Hagiwara, T. Kawahara, Y. Yamanishi, and F. Arai, "Driving Method of Microtool by Horizontally Arranged Permanent Magnets for Single Cell Manipulation," *Applied Physics Letters* 97, no. 1 (2010): 013701, https://doi.org/10.1063/1.3459040.

97. P. Valdastri, E. Sinibaldi, S. Caccavaro, G. Tortora, A. Menciassi, and P. Dario, "A Novel Magnetic Actuation System for Miniature Swimming Robots," *IEEE Transactions on Robotics* 27, no. 4 (2011): 769–779, https://doi.org/10.1109/TRO.2011.2132910.

98. A. W. Mahoney and J. J. Abbott, "Generating Rotating Magnetic Fields With a Single Permanent Magnet for Propulsion of Untethered Magnetic Devices in a Lumen," *IEEE Transactions on Robotics* 30, no. 2 (2014): 411–420, https://doi.org/10.1109/TRO.2013.2289019.

99. A. W. Mahoney and J. J. Abbott, "Five-degree-of-freedom Manipulation of an Untethered Magnetic Device in Fluid Using a Single Permanent Magnet With Application in Stomach Capsule Endoscopy," *International Journal of Robotics Research* 35, no. 1–3 (2016): 129–147, https://doi.org/10.1177/0278364914558006.

100. G. Pittiglio, M. Brockdorff, T. Da Veiga, J. Davy, J. H. Chandler, and P. Valdastri, "Collaborative Magnetic Manipulation via Two Robotically Actuated Permanent Magnets," *IEEE Transactions on Robotics* 39, no. 2 (2023): 1407–1418, https://doi.org/10.1109/TRO.2022.3209038.

101. S. E. Wright, A. W. Mahoney, K. M. Popek, and J. J. Abbott, "The Spherical-Actuator-Magnet Manipulator: A Permanent-Magnet Robotic End-Effector," *IEEE Transactions on Robotics* 33, no. 5 (2017): 1013–1024, https://doi.org/10.1109/TRO.2017.2694841.

102. Z. Yang, L. Liu, X. Li, J. Li, Y. Jiao, and Y. Cui, "Development and Control of a Dual-Mode Magnetic Intravascular Ultrasound Robot for Imaging in Tortuous Blood Vessels," *IEEE Transactions on Mechatronics* 30 (2024): 1–12, https://doi.org/10.1109/TMECH.2024.3392243.

103. Z. Koszowska, M. Brockdorff, T. da Veiga, et al., "Independently Actuated Soft Magnetic Manipulators for Bimanual Operations in Confined Anatomical Cavities," *Advanced Intelligent Systems* 6, no. 2 (2024): 2300062, https://doi.org/10.1002/aisy.202300062.

104. E. S. Gang, B. L. Nguyen, Y. Shachar, et al., "Dynamically Shaped Magnetic Fields: Initial Animal Validation of a New Remote Electrophysiology Catheter Guidance and Control System," *Circulation: Arrhythmia and Electrophysiology* 4, no. 5 (2011): 770–777, https://doi.org/10.1161/CIRCEP.110.959692.

105. W. Lee, J. Nam, J. Kim, E. Jung, N. Kim, and G. Jang, "Steering, Tunneling, and Stent Delivery of a Multifunctional Magnetic Catheter Robot to Treat Occlusive Vascular Disease," *IEEE Transactions on Industrial Electronics* 68, no. 1 (2021): 391–400, https://doi.org/10.1109/TIE.2020.2965480.

106. D. Liu, X. Liu, Z. Chen, et al., "Magnetically Driven Soft Continuum Microrobot for Intravascular Operations in Microscale," *Cyborg and Bionic Systems* 2022 (2022): 2022–9850832, https://doi.org/10.34133/2022/9850832.

107. C. M. Heunis, K. J. Behrendt, E. E. G. Hekman, C. Moers, J.-P. P. M. D. Vries, and S. Misra, "Design and Evaluation of a Magnetic Rotablation Catheter for Arterial Stenosis," *IEEE* 27, no. 3 (2022): 1761–1772, https://doi.org/10.1109/TMECH.2021.3092608.

108. C. Fischer, Q. Boehler, and B. J. Nelson, "Using Magnetic Fields to Navigate and Simultaneously Localize Catheters in Endoluminal Environments," *IEEE Robotics and Automation Letters* 7, no. 3 (2022): 7217–7223, https://doi.org/10.1109/LRA.2022.3181420.

109. H. Yang, Z. Yang, D. Jin, et al., "Magnetic Micro-driller System for Nasolacrimal Duct Recanalization," *IEEE Robotics and Automation Letters* 7, no. 3 (2022): 7367–7374, https://doi.org/10.1109/LRA.2022.3182105.

110. J. Yu, D. Jin, K.-F. Chan, Q. Wang, K. Yuan, and L. Zhang, "Active Generation and Magnetic Actuation of Microrobotic Swarms in Bio-Fluids," *Nature Communications* 10, no. 1 (2019): 5631, https://doi.org/10.1038/s41467-019-13576-6.

111. L. Yang, J. Jiang, X. Gao, Q. Wang, Q. Dou, and L. Zhang, "Autonomous Environment-Adaptive Microrobot Swarm Navigation Enabled by Deep Learning-Based Real-Time Distribution Planning," *Nature Machine Intelligence* 4, no. 5 (2022): 480–493, https://doi.org/10.1038/s42256-022-00482-8.

112. T. Xu, C. Huang, Z. Lai, and X. Wu, "Independent Control Strategy of Multiple Magnetic Flexible Millirobots for Position Control and Path Following," *IEEE Transactions on Robotics* 38, no. 5 (2022): 2875–2887, https://doi.org/10.1109/TRO.2022.3157147.

113. Q. Wang, S. Yang, and L. Zhang, "Magnetic Actuation of a Dynamically Reconfigurable Microswarm for Enhanced Ultrasound Imaging Contrast," *IEEE* 27, no. 6 (2022): 4235–4245, https://doi.org/10.1109/TMECH.2022.3151983.

114. Y. Liu, H. Chen, Q. Zou, X. Du, Y. Wang, and J. Yu, "Automatic Navigation of Microswarms for Dynamic Obstacle Avoidance," *IEEE Transactions on Robotics* 39, no. 4 (2023): 2770–2785, https://doi.org/10.1109/TRO.2023.3263773.

115. M. Cai, Z. Qi, Y. Cao, et al., "Performance-Guided Rotating Magnetic Field Control in Large Workspaces With Reconfigurable Electromagnetic Actuation System," *IEEE Transactions on Robotics* 40 (2024): 4117–4131, https://doi.org/10.1109/TRO.2024.3453768.

116. T. Xu, G. Hwang, N. Andreff, and S. Regnier, "Planar Path Following of 3-D Steering Scaled-Up Helical Microswimmers," *IEEE Transactions on Robotics* 31, no. 1 (2015): 117–127, https://doi.org/10.1109/TRO.2014.2380591.

117. R. Dreyfus, Q. Boehler, and B. J. Nelson, "A Simulation Framework for Magnetic Continuum Robots," *IEEE Robotics and Automation Letters* 7, no. 3 (2022): 8370–8376, https://doi.org/10.1109/LRA.2022.3187249.

118. J. Sikorski, A. Denasi, G. Bucchi, S. Scheggi, and S. Misra, "Vision-Based 3-D Control of Magnetically Actuated Catheter Using BigMag—An Array of Mobile Electromagnetic Coils," *IEEE* 24, no. 2 (2019): 505–516, https://doi.org/10.1109/TMECH.2019.2893166.

119. A. Azizi, C. C. Tremblay, K. Gagné, and S. Martel, "Using the Fringe Field of a Clinical MRI Scanner Enables Robotic Navigation of Tethered Instruments in Deeper Vascular Regions," *Science Robotics* 4, no. 36 (2019): eaax7342, https://doi.org/10.1126/scirobotics.aax7342.

120. M. E. Tiryaki, Y. G. Elmacıoğlu, and M. Sitti, "Magnetic Guidewire Steering at Ultrahigh Magnetic Fields," *Science Advances* 9, no. 17 (2023): eadg6438, https://doi.org/10.1126/sciadv.adg6438.

121. O. Erin, M. Boyvat, M. E. Tiryaki, M. Phelan, and M. Sitti, "Magnetic Resonance Imaging System–Driven Medical Robotics," *Advanced Intelligent Systems* 2, no. 2 (2020): 1900110, https://doi.org/10.1002/aisy.201900110.

122. G.-Z. Yang, J. Cambias, K. Cleary, et al., "Medical Robotics—Regulatory, Ethical, and Legal Considerations for Increasing Levels of Autonomy," *Science Robotics* 2, no. 4 (2017): eaam8638, https://doi.org/10.1126/scirobotics.aam8638.

123. T. Haidegger, "Autonomy for Surgical Robots: Concepts and Paradigms," *IEEE Transactions on Medical Robotics and Bionics* 1, no. 2 (2019): 65–76, https://doi.org/10.1109/TMRB.2019.2913282.

124. A. A. Nazari, K. Zareinia, and F. Janabi-Sharifi, "Visual Servoing of Continuum Robots: Methods, Challenges, and Prospects," *International Journal of Medical Robotics* 18, no. 3 (2022): e2384, https://doi.org/10.1002/rcs.2384.

125. M. Richter, M. Kaya, J. Sikorski, L. Abelmann, V. Kalpathy Venkiteswaran, and S. Misra, "Magnetic Soft Helical Manipulators With Local Dipole Interactions for Flexibility and Forces," *Soft Robotics* 10, no. 3 (2023): 647–659, https://doi.org/10.1089/soro.2022.0031.

126. T. Krings, J. Finney, P. Niggemann, et al., "Magnetic versus Manual Guidewire Manipulation in Neuroradiology: In Vitro Results," *Neuroradiology* 48, no. 6 (2006): 394–401, https://doi.org/10.1007/s00234-006-0082-3.

127. X. Li, W. Yu, J. Liu, et al., "A Mechanics Model of Hard-Magnetic Soft Rod With Deformable Cross-Section under Three-Dimensional Large Deformation," *International Journal of Solids and Structures* 279 (2023): 112344, https://doi.org/10.1016/j.ijsolstr.2023.112344.

128. Y. Liu, T. G. Mohanraj, M. R. Rajebi, L. Zhou, and F. Alambeigi, "Multiphysical Analytical Modeling and Design of a Magnetically Steerable Robotic Catheter for Treatment of Peripheral Artery Disease," *IEEE* 27, no. 4 (2022): 1873–1881, https://doi.org/10.1109/TMECH.2022.3174520.

129. Y. Kim, E. Genevriere, P. Harker, et al., "Telerobotically Controlled Magnetic Soft Continuum Robots for Neurovascular Interventions," in *2022 International Conference on Robotics and Automation (ICRA)* (IEEE, 2022), 9600–9606, https://doi.org/10.1109/ICRA46639.2022.9812168.

130. Y. Kim, E. Genevriere, P. Harker, et al., "Telerobotic Neurovascular Interventions With Magnetic Manipulation," *Science Robotics* 7, no. 65 (2022): eabg9907, https://doi.org/10.1126/scirobotics.abg9907.

131. S. Xu, B. Chen, S. Fu, X. Wu, S. Du, and T. Xu, "An Automatic Magnetically Robotic System Using a Double-Loop Stable Control Method for Guidewire Steering," *IEEE* (2024): 1–12, https://doi.org/10.1109/TMECH.2024.3477594.

132. J. Tan, J. Xue, X. Yang, et al., "Model-free and Uncalibrated Visual-Feedback Control of Magnetically-Actuated Flexible Endoscopes," in *2022 IEEE/RSJ International Conference on Intelligent Robots and Systems (IROS)* (IEEE, 2022), 5930–5936, https://doi.org/10.1109/IROS47612.2022.9982055

133. D. Chathuranga, P. Lloyd, J. H. Chandler, R. A. Harris, and P. Valdastri, "Assisted Magnetic Soft Continuum Robot Navigation via Rotating Magnetic Fields," *IEEE Robotics and Automation Letters* 9, no. 1 (2024): 183–190, https://doi.org/10.1109/LRA.2023.3331292.

134. J. Wu, N. Jiao, D. Lin, et al., "Dual-Responsive Nanorobot-Based Marsupial Robotic System for Intracranial Cross-Scale Targeting Drug

Delivery," *Advanced Materials* 36, no. 9 (2024): 2306876, https://doi.org/10.1002/adma.202306876.

135. J. Fan, S. Ren, B. Han, et al., "Magnetic Fiber Robots With Multiscale Functional Structures at the Distal End," *Advanced Functional Materials* 34, no. 12 (2024): 2309424, https://doi.org/10.1002/adfm.202309424.

136. S. Yuan, C. Xu, B. Cui, et al., "Motor-free Telerobotic Endomicroscopy for Steerable and Programmable Imaging in Complex Curved and Localized Areas," *Nature Communications* 15, no. 1 (2024): 7680, https://doi.org/10.1038/s41467-024-51633-x.

137. R. Li, J. Wang, X. Zhao, et al., "Small-scale Magnetic Soft Robotic Catheter for In-Situ Biomechanical Force Sensing," *Biosensors and Bioelectronics* 270 (2025): 116977, https://doi.org/10.1016/j.bios.2024.116977.

138. S. Fu, B. Chen, J. Han, et al., "A Magnetically Controlled Guidewire Robot System With Steering and Propulsion Capabilities for Vascular Interventional Surgery," *Advanced Intelligent Systems* 5, no. 11 (2023): 2300267, https://doi.org/10.1002/aisy.202300267.

139. J. Kim, S. E. Chung, S.-E. Choi, H. Lee, J. Kim, and S. Kwon, "Programming Magnetic Anisotropy in Polymeric Microactuators," *Nature Materials* 10, no. 10 (2011): 747–752, https://doi.org/10.1038/nmat3090.

140. J. Tang, Q. Yin, Y. Qiao, and T. Wang, "Shape Morphing of Hydrogels in Alternating Magnetic Field," *ACS Applied Materials and Interfaces* 11, no. 23 (2019): 21194–21200, https://doi.org/10.1021/acsami.9b05742.

141. B. A. Bernevig, C. Felser, and H. Beidenkopf, "Progress and Prospects in Magnetic Topological Materials," *Nature* 603, no. 7899 (2022): 41–51, https://doi.org/10.1038/s41586-021-04105-x.

142. Y. Lee, F. Koehler, T. Dillon, et al., "Magnetically Actuated Fiber-Based Soft Robots," *Advanced Materials* 35, no. 38 (2023): 2301916, https://doi.org/10.1002/adma.202301916.

143. Y. Kim, H. Yuk, R. Zhao, S. A. Chester, and X. Zhao, "Printing Ferromagnetic Domains for Untethered Fast-Transforming Soft Materials," *Nature* 558, no. 7709 (2018): 274–279, https://doi.org/10.1038/s41586-018-0185-0.

144. T. Xu, J. Zhang, M. Salehizadeh, O. Onaizah, and E. Diller, "Millimeter-scale Flexible Robots With Programmable Three-Dimensional Magnetization and Motions," *Science Robotics* 4, no. 29 (2019): eaav4494, https://doi.org/10.1126/scirobotics.aav4494.

145. R. Xie, Y. Cao, R. Sun, et al., "Magnetically Driven Formation of 3D Freestanding Soft Bioscaffolds," *Science Advances* 10, no. 5 (2024): eadl1549, https://doi.org/10.1126/sciadv.adl1549.

146. P. Wu, T. Yu, M. Chen, N. Kang, and M. E. Mansori, "Electrically/Magnetically Dual-Driven Shape Memory Composites Fabricated by Multi-Material Magnetic Field-Assisted 4D Printing," *Advanced Functional Materials* 34, no. 27 (2024): 2314854, https://doi.org/10.1002/adfm.202314854.

147. J. Liu, R. Zhuang, D. Zhou, X. Chang, and L. Li, "Design and Manufacturing of Micro/nanorobots," *International Journal of Extreme Manufacturing* 6, no. 6 (2024): 062006, https://doi.org/10.1088/2631-7990/ad720f.

148. B. Wang, K. F. Chan, J. Yu, et al., "Reconfigurable Swarms of Ferromagnetic Colloids for Enhanced Local Hyperthermia," *Advanced Functional Materials* 28, no. 25 (2018): 1705701, https://doi.org/10.1002/adfm.201705701.

149. O. Youssefi and E. Diller, "Contactless Robotic Micromanipulation in Air Using a Magneto-Acoustic System," *IEEE Robotics and Automation Letters* 4, no. 2 (2019): 1580–1586, https://doi.org/10.1109/LRA.2019.2896444.

150. M. Sun, B. Sun, M. Park, et al., "Individual and Collective Manipulation of Multifunctional Bimodal Droplets in Three Dimensions," *Science Advances* 10, no. 29 (2024): eadp1439, https://doi.org/10.1126/sciadv.adp1439.

151. J. Liu, S. Wang, S. Huang, et al., "Magnetic and Radio Frequency Dual-Responsive Shape-Programmable Robots for Adaptive Aneurysm Embolization," *Cell Rep. Phys. Sci.* 5, no. 9 (2024): 102160, https://doi.org/10.1016/j.xcrp.2024.102160.

152. S. Ernst, F. Ouyang, C. Linder, et al., "Initial Experience With Remote Catheter Ablation Using a Novel Magnetic Navigation System: Magnetic Remote Catheter Ablation," *Circulation* 109, no. 12 (2004): 1472–1475, https://doi.org/10.1161/01.CIR.0000125126.83579.1B.

153. X. Yan, Q. Zhou, M. Vincent, et al., "Multifunctional Biohybrid Magnetite Microrobots for Imaging-Guided Therapy," *Science Robotics* 2, no. 12 (2017): eaaq1155, https://doi.org/10.1126/scirobotics.aaq1155.

154. J. C. Norton, P. R. Slawinski, H. S. Lay, et al., "Intelligent Magnetic Manipulation for Gastrointestinal Ultrasound," *Science Robotics* 4, no. 31 (2019): eaav7725, https://doi.org/10.1126/scirobotics.aav7725.

155. Q. Wang, B. Wang, J. Yu, K. Schweizer, B. J. Nelson, and L. Zhang, "Reconfigurable Magnetic Microswarm for Thrombolysis Under Ultrasound Imaging," in *2020 IEEE International Conference On Robotics And Automation (ICRA)*, (IEEE, 2020), 10285–10291, https://doi.org/10.1109/ICRA40945.2020.9197432.

156. Z. Yang, L. Yang, M. Zhang, C. Zhang, S. C. H. Yu, and L. Zhang, "Ultrasound-Guided Catheterization Using a Driller-Tipped Guidewire With Combined Magnetic Navigation and Drilling Motion," *IEEE Transactions on Mechatronics* 27, no. 5 (2022): 2829–2840, https://doi.org/10.1109/TMECH.2021.3121267.

157. Z. Yang, L. Yang, M. Zhang, N. Xia, and L. Zhang, "Ultrasound-Guided Wired Magnetic Microrobot With Active Steering and Ejectable Tip," *IEEE Transactions on Industrial Electronics* 70, no. 1 (2023): 614–623, https://doi.org/10.1109/TIE.2022.3153809.

158. E. Ren, J. Hu, Z. Mei, et al., "Water-Stable Magnetic Lipiodol Micro-Droplets as a Miniaturized Robotic Tool for Drug Delivery," *Advanced Materials* 37, no. 3 (2024): 2412187, https://doi.org/10.1002/adma.202412187.